**SANDIA REPORT**
SAND87—1449 • UC—80
Unlimited Release
Printed August 1987

# The Effect of Maximum-Allowable Payload Temperature on the Mass of a Multimegawatt Space-Based Platform



Dean Dobranich

**Prepared by**
**Sandia National Laboratories**
**Albuquerque, New Mexico 87185 and Livermore, California 94550**
**for the United States Department of Energy**
**under Contract DE-AC04-76DP00789**

Issued by Sandia National Laboratories, operated for the United States Department of Energy by Sandia Corporation.



Printed in the United States of America
Available from
National Technical Information Service
U.S. Department of Commerce
5285 Port Royal Road
Springfield, VA 22161

NTIS price codes
Printed copy: A03
Microfiche copy: A01

SAND87-1449
Unlimited Release
Printed August 1987

Distribution
Category UC-80

# THE EFFECT OF MAXIMUM-ALLOWABLE PAYLOAD TEMPERATURE ON THE MASS OF A MULTIMEGAWATT SPACE-BASED PLATFORM

Dean Dobranich
Advanced Nuclear Power Systems Safety Division
Sandia National Laboratories
Albuquerque, New Mexico 87185

## ABSTRACT

Calculations were performed to determine the mass of a space-based platform as a function of the maximum-allowed operating temperature of the electrical equipment within the platform payload. Two computer programs were used in conjunction to perform these calculations. The first program was used to determine the mass of the platform reactor, shield, and power conversion system. The second program was used to determine the mass of the main and secondary radiators of the platform. The main radiator removes the waste heat associated with the power conversion system and the secondary radiator removes the waste heat associated with the platform payload. These calculations were performed for both Brayton and Rankine cycle platforms with two different types of payload cooling systems: a pumped-loop system (a heat exchanger with a liquid coolant) and a refrigerator system. The results indicate that increases in the maximum-allowed payload temperature offer significant platform mass savings for both the Brayton and Rankine cycle platforms with either the pumped-loop or refrigerator payload cooling systems. Therefore, with respect to platform mass, the development of high temperature electrical equipment would be advantageous.

CONTENTS

# 1.0 INTRODUCTION

Proposed space-based platforms will require tens of megawatts of thermal power to perform their desired function. The cost associated with the launching of these multimegawatt (MMW) platforms is directly related to the platform mass. Therefore, estimating the mass of these conceptual platforms is of considerable interest. A primary part of such a platform is the payload, which consists of electrical equipment such as radios, radars, computers, and guidance systems. The consumption of electrical power by this equipment will result in the generation of large amounts of waste heat which must be removed to keep the operating temperature of the equipment below some acceptable limit. The value of this temperature limit strongly affects the mass of the platform because it influences the size of the "secondary" radiator required for waste heat rejection to space. This radiator can account for a significant fraction of the platform mass and is in addition to the main radiator associated with removal of the waste heat of the platform thermal-to-electric power conversion system.

Two separate computer programs were used in conjunction to estimate the mass of a MMW platform as a function of the maximum-allowable payload operating temperature. The first computer program [1] determines the mass of a platform required to produce a specified quantity of electric power for a specified time. The program includes mass estimates for the thermal power source (a nuclear reactor), the reactor shield, the power conversion system (either a Brayton or Rankine thermodynamic cycle), and the main radiator. The mass of the secondary radiator is not included in this platform mass estimate. In addition to the platform mass, the first program determines the required amount of thermal power and the main radiator operating temperature. This output serves as input to the second program [2], which is used to determine the secondary radiator size as a function of payload operating temperature. In determining the secondary radiator size, the second program accounts for the radiative influence of the main radiator, the power conditioning unit (PCU), and the payload. These relatively hot platform structures contribute to the thermal background associated with the ultimate heat sink for waste heat (i.e., space).

Cooling of the payload can be accomplished using either a pumped-loop cooling system or a refrigerator. The pumped-loop cooling system uses a liquid working fluid flowing through the payload without phase change. The working fluid is cooled as it flows through the secondary radiator which consists of heat pipes. With this type of payload cooling, the radiator temperature cannot exceed the temperature of the payload. Thus,

higher allowable payload temperatures allow waste heat rejection at higher temperatures. Because of the fourth power dependence of temperature on radiator area, an increase in radiator temperature can significantly reduce the size of the secondary radiator.

If a refrigerator is used to cool the payload, phase change of the working fluid occurs as it passes through the payload. The resulting vapor working fluid is then increased in both temperature and pressure by a compressor before passing through the heat pipe secondary radiator. Thus, refrigerator cooling of the payload allows rejection of the waste heat at a temperature above that of the payload. However, the working fluid must be at a temperature below that of the payload as it cools the payload. Increasing the payload allowable temperature therefore can result in a higher coefficient of performance for the refrigerator. This in turn decreases the additional power demands of the refrigerator and results in lower platform mass.

An additional (though less significant) benefit associated with higher allowable payload operating temperatures exists. Any waste heat generated by the payload that is not removed actively by either of the aforementioned cooling systems must be removed radiatively. If the allowable payload temperature is decreased, more waste heat must be removed actively, resulting in a larger secondary radiator. Contrariwise, higher allowable payload temperatures reduce the amount of waste heat to be removed actively.

Calculations were performed to estimate total platform mass for platforms using both Brayton and Rankine cycle power conversion systems. Platform mass estimates were also made for each system for both types of payload cooling systems (i.e., pumped loop and refrigerator). These mass estimates were determined as a function of the maximum-allowable payload operating temperature to demonstrate the benefit that can be realized by the development of high temperature electrical equipment. This report documents the results of these calculations.

## 2.0 APPROACH AND ASSUMPTIONS

As mentioned in the introduction, two separate computer programs were used in conjunction to determine the total platform mass. Detailed descriptions of these two programs can be found in References 1 and 2. Brief descriptions of the two programs are included here for convenience. These descriptions are followed by a description of the assumptions made to use these two programs for calculating platform mass.

The first program, referred to in this report as the MMW systems program, provides an estimate of the total mass of MMW space-based platforms with the exception of the secondary radiator mass. The secondary radiator is necessary for the removal of the waste heat associated with active cooling of the electrical equipment within the payload of the platform. The MMW systems program can be used for a platform using either a Brayton cycle (without a regenerator) or Rankine cycle (direct or indirect) power conversion system. The Brayton cycle platform consists of a helium-cooled reactor with shield, a power conversion system, and a main radiator. The power conversion system is comprised of a turbine, a compressor, a generator, and a power conditioning unit. Within the program, the temperature and pressure ratios of the Brayton thermodynamic cycle are optimized to produce the minimum platform mass. The Rankine cycle platform consists of a liquid-metal cooled reactor with shield, a power conversion system, and a main radiator. The power conversion system is comprised of a vapor separator, a condenser, a turbine, a generator, and a power conditioning unit. The program optimizes the condenser temperature to produce the minimum platform mass.

The second program, referred to in this report as the MMW platform heat transfer program, provides an estimate of the main radiator and secondary radiator geometric areas along with the temperatures of the PCU and payload. The sizes of the two radiators depend on their proximity to each other and to the other platform structures. Also, the size of the secondary radiator depends on the temperature of the payload, which is initially unknown. Thus, an iterative solution scheme is employed.

Figure 2.1 shows a schematic of the platform structures modeled for the radiative heat transfer calculations. The PCU and payload shells provide meteoroid protection and are coupled radiatively and conductively to the PCU and payload, respectively. The user can specify conduction parameters between the PCU and payload and their shells or the desired temperature difference between them. (Heat pipes can provide essentially isothermal heat transfer to the shells if sufficient space exists to accommodate the heat transfer requirements.)

The two opposing flat disks representing the main and secondary radiators probably do not represent the optimal radiator configuration; this configuration was chosen for modeling simplicity and to demonstrate that the position of the platform components relative to each other strongly affects the radiant heat transfer calculations. (The optimal configuration will depend on factors other than just the heat transfer considerations such as platform stability, maneuverability, survivability, and structural considerations.) The separation distance between the platform structures can be selected by the program user; all view factors for the radiant heat transfer calculations are determined automatically by the program.

Figure 2.2 shows the relationship between the secondary radiator temperature and the payload pumped-loop cooling system working fluid temperature. Higher payload operating temperatures allow higher secondary radiator heat rejection temperatures. If a refrigerator is used, the rejection temperature can be higher than the payload temperature but the working fluid temperature must still be below the temperature of the payload. Modeling all the electrical equipment as a single payload is based on the simplification that the different electronic components within the payload operate at the same temperature. In reality, each component will have different temperature limitations and may even require its own radiator.

The procedure for determining the total platform mass is summarized as follows. First, the MMW systems program is used to determine the platform mass, which does not include an estimate of the secondary radiator mass. The mass of the main radiator is subtracted from this platform mass estimate because the systems program does not account for the radiant interaction between the main radiator and the other platform structures when determining the main radiator size. The resulting mass is referred to as the balance-of-platform (BOP) mass.

The systems program also determines the operating temperature of the main radiator (inlet and outlet radiator temperature for the Brayton cycle platform) and the amount of thermal power required to produce the specified electrical power demands. This output is then used as input to the MMW platform heat transfer program. This program calculates the required area of the main and secondary radiators and the payload temperature. Different payload temperatures are achieved by varying the amount of waste heat removed actively by the payload cooling system (pumped loop or refrigerator). The main and secondary radiator geometric areas are then multiplied by a specified mass per unit area value to arrive at their respective masses. These radiator masses are added to the BOP mass to arrive at the total platform mass as a function of the calculated payload temperature.

If a refrigerator is used to cool the payload, an additional mass is added to account for the mass of the vapor working fluid compressor. This mass is determined by multiplying the refrigerator electrical power demand (calculated by the platform heat transfer program) by a specified mass per electric power value. After the additional electric power required to run the refrigerator is determined, it is added to the original platform electric power and the systems program is rerun. This results in a larger reactor thermal power and may change the optimum operating temperature of the main radiator. Thus, iteration between the two programs is required to determine the platform mass if a refrigerator is used to cool the payload.

To use each of the two programs, the values of many input parameters must be assumed. A few of these values are treated parametrically, however, most of them are assigned some "base case" value that is used for all calculations. Both Brayton cycle and Rankine cycle platform base cases are defined for the platform mass analyses. The input parameters for these base cases for the MMW systems program are listed in Tables 2.1 and 2.2. (Further description of the reactor parameters is provided in [3]; this reference documents the RSMASS computer code that is used as a subroutine within the MMW systems program to calculate the mass of the reactor and shield.) Information required to use the platform heat transfer program is summarized in Table 2.3 followed by a brief description of some of the more important parameters.

Table 2.1

Systems Program Base Case Input - Brayton Cycle

| | |
|---|---|
| Platform Electric Power | 10 MW |
| Operating Time | 1 year |
| Turbine Inlet Temperature | 1500 K |
| Turbine Inlet Pressure | 2.7 MPa |
| Helium Compressor Efficiency | 0.85 |
| Generator Efficiency | 0.95 |
| Power Conditioning Efficiency | 0.95 |
| Fractional Fuel Enrichment | 0.93 |
| Critical Compact Mass | 2.0 kg |
| Critical Mass Correction Factor | 3.1 |
| Fuel plus Moderator Volume Fraction | 0.292 |
| Fuel Power Density | 0.39 MW/kg |
| Fractional Core Pressure Drop | 0.01 |
| Fuel Burnup Fraction Limit | 0.25 |
| Moderator-To-Fuel Ratio | 20.0 |
| Moderator Molecular Weight | 93 |
| Moderator Density | 5610 $kg/m^3$ |
| Structure-To-Fuel and Moderator Ratio | 1.966 |
| Structure Density | 6071 $kg/m^3$ |
| Core Removal Cross Section | 0.1465 $cm^{-1}$ |

| | |
|---|---|
| Core Gamma Attenuation Cross Section | 0.379 $cm^{-1}$ |
| Allowed Payload Neutron Dose | 5.0E16 nvt |
| Payload-to-Shield Separation Distance | 25 m |
| Protection Cone Half Angle | 15 degrees |
| Neutron Shield Material | LiH |
| Allowed Payload Gamma Dose | 1.0E7 R |
| Number of Turbines | 4 |
| Turbine Material | Superalloy |
| Maximum Blade Temperature | 1000 K |
| Maximum Turbine Speed | 50,000 rpm |
| Work Coefficient | 1.2 |
| Radiator Emissivity | 0.88 |

Table 2.2

Systems Program Base Case Input - Direct Rankine Cycle

| | |
|---|---|
| Platform Electric Power | 10 MW |
| Operating Time | 1 year |
| Reactor Outlet Temperature | 1200 K |
| Turbine Efficiency | 0.85 |
| Generator Efficiency | 0.95 |
| Power Conditioning Efficiency | 0.95 |
| Fractional Fuel Enrichment | 0.7 |
| Critical Compact Mass | 28.0 kg |
| Fuel Density | 13600 $kg/m^3$ |
| Critical Mass Correction Factor | 1.0 |
| Fuel plus Moderator Volume Fraction | 0.6 |
| Fuel Power Density | 5.0 MW/kg |
| Fuel Burnup Fraction Limit | 0.065 |
| Moderator-To-Fuel Ratio | 0.0 |
| Structure-To-Fuel and Moderator Ratio | 0.6 |
| Structure Density | 7300 $kg/m^3$ |
| Core Removal Cross Section | 0.14 $cm^{-1}$ |
| Core Gamma Attenuation Cross Section | 1.0 $cm^{-1}$ |
| Allowed Payload Neutron Dose | 5.0E16 nvt |
| Payload-to-Shield Separation Distance | 25 m |
| Protection Cone Half Angle | 15 degrees |
| Neutron Shield Material | LiH |
| Allowed Payload Gamma Dose | 1.0E7 R |
| Radiator Emissivity | 0.88 |

Table 2.3

Platform Heat Transfer Program Base Case Input

| | |
|---|---|
| Main Radiator Emissivity | 0.88 |
| Secondary Radiator Emissivity | 0.88 |
| PCU Shell Emissivity | 0.9 |
| Payload Shell Emissivity | 0.9 |
| PCU Emissivity | 0.8 |

| | |
|---|---|
| Payload Emissivity | 0.8 |
| PCU-to-Shell Temperature Difference | 2 K |
| Payload-to-Shell Temperature Difference | 2 K |
| PCU-to-Main Radiator Separation Distance | 1 m |
| Payload-to-Sec Radiator Separation Distance | 1 m |
| Main-to-Sec Radiator Separation Distance | 250 m |
| PCU Shell Area/Platform Electric Power | 16 $m^2$/MWe |
| Payload Shell Area/Platform Electric Power | 30 $m^2$/MWe |
| PCU Length-to-Diameter Ratio | 1.5 |
| Payload Length-to-Diameter Ratio | 1.5 |
| PCU Efficiency | 0.95 |
| Payload Efficiency | 0.01 |
| Temperature of Space | 250 K |
| Fraction of Carnot COP (for refrigerator) | 0.75 |
| Minimum Approach Temperature ($\Delta T_{min}$) | 20 K |
| Secondary Radiator Temperature Drop | 50 K |
| Refrigerator Specific Mass | 1.0 kg/kWe |
| Main Radiator Mass per Area (Brayton) | 6 $kg/m^2$ |
| Main Radiator Mass per Area (Rankine) | 8 $kg/m^2$ |
| Secondary Radiator Mass per Area (T<650 K) | 5 $kg/m^2$ |
| Secondary Radiator Mass per Area (T>650 K) | 8 $kg/m^2$ |

The payload efficiency of 0.01 means that 99% of the electric power used by the payload is converted to waste heat. (Calculations with a payload efficiency of 0.5 were also performed.) The temperature of space represents an average temperature for a spacecraft in a low equatorial earth orbit. For higher orbits and for polar orbits, the spacecraft would have a greater exposure to the sun, resulting in a higher effective space temperature. This would lead to larger main and secondary radiator areas, especially for the secondary radiator which operates at relatively low temperatures. Thus, use of the space temperature representative of low earth orbit is optimistic with respect to radiator mass (i.e., higher space temperatures result in larger radiators).

A Carnot refrigerator is one that has the maximum thermodynamically possible COP. This COP is determined based on the temperatures where heat is added and removed from the working fluid. To determine the COP of a real refrigerator with mechanical irreversible losses, the Carnot COP is multiplied by 0.75. This is about the best one can expect for a refrigerator; lower values of this multiplier result in the need for more power and thus heavier platforms.

The minimum approach temperature and the secondary radiator temperature drop were arbitrarily selected as 20 K and 50 K, respectively. The minimum approach temperature, as indicated on Figure 2.2, is the minimum temperature difference between the payload and the working fluid. Figure 2.2 also shows that the temperature drop across the secondary radiator is equal to the temperature drop across the payload heat exchanger. The mean

temperature differential between the payload and the working fluid is 45 K. This temperature differential is used for both the pumped-loop and the refrigerator payload cooling systems.

A compressor is expected to weigh more than a pump that uses an incompressible working fluid as in the pumped-loop payload cooling system. Therefore, the refrigerator specific mass is included to account for the mass of the refrigerator compressor. Larger values for the refrigerator specific mass result in heavier platforms.

The radiator mass per area value for the Rankine cycle platform main radiator is larger than the Brayton cycle main radiator because it operates at a higher temperature and thus requires inherently heavier high-temperature materials. The secondary radiator operates at very low temperatures and thus does not require heavy materials unless a refrigerator is used to reject heat at a high temperature. The radiator mass per area values selected for use in these analyses are at the lower limit of what is reasonably achievable; larger, more realistic values will result in heavier radiators.

The maximum-allowable payload operating temperature has the largest effect on the size of the secondary radiator and on the amount of power (both thermal and electric) needed to run a refrigerator. Increasing the payload operating temperature significantly reduces the secondary radiator size. Also, if a refrigerator is used, less power is needed if higher payload operating temperatures are allowed because of the increase in the refrigerator COP. An effort was made to select values for the heat transfer program (for all input parameters) that result in the minimum secondary radiator size and the minimum power demands if a refrigerator is used. This diminishes the relative mass savings that can be achieved by using high temperature electrical components in the payload. Conversely, choosing less optimistic values would emphasize the benefit of high payload temperatures. As will be demonstrated, even when optimistic input values are used, the benefits of high temperature electrical equipment can be substantial.

As indicated by the long list of input variables, many assumptions had to be made concerning the conceptual space platforms before mass calculations could be made. Because of the many uncertainties associated with an analysis of this kind, some variables were treated parametrically to demonstrate their relative effect on the platform mass results. However, parametric treatment of all of the variables would, of course, be prohibitive. The results presented in this report are intended to indicate the general trends and dependences; more precise mass calculations cannot be performed until detailed design information becomes available.

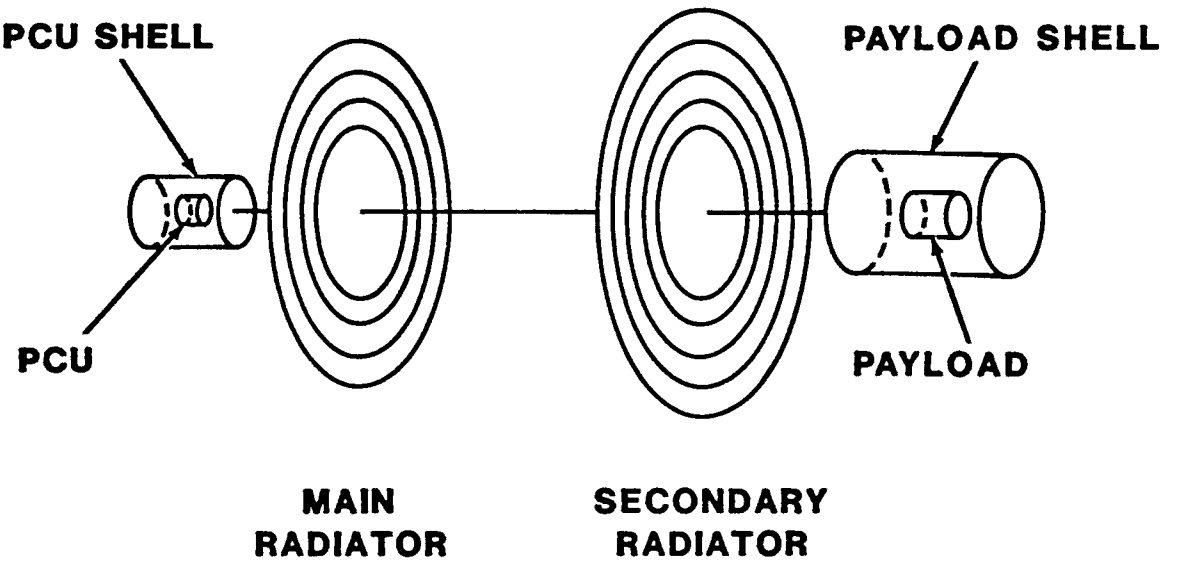


Figure 2.1 MMW Platform Structures

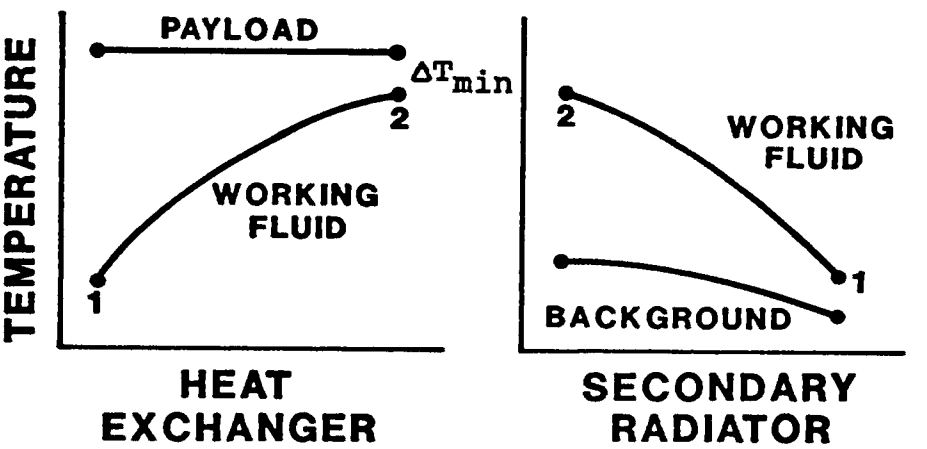


Figure 2.2 Relationship Between Secondary Radiator and Working Fluid Temperatures

## 3.0 BRAYTON CYCLE PLATFORM RESULTS

### 3.1 Pumped-Loop Payload Cooling System

Platform mass calculations were performed first for the Brayton cycle platforms that used the pumped-loop payload cooling system as opposed to a refrigerator. First, the MMW systems program was used to find the BOP mass; the results of this program for the base case platform are summarized in Table 3.1.1. (The miscellaneous mass for the platform is calculated by the systems program as 10% of the reactor, shield, main radiator, and power conversion system masses.)

Table 3.1.1

Brayton Cycle Systems Program Results (Base Case)

| | |
|---|---|
| Thermal Power | 46 MW |
| Main Radiator Inlet Temperature | 810 K |
| Main Radiator Outlet Temperature | 369 K |
| Reactor Mass | 5591 kg |
| Shield Mass | 4564 kg |
| Power Conversion System Mass | 5960 kg |
| Miscellaneous Mass | 5890 kg |
| Total BOP Mass | 22005 kg |

Next, the platform heat transfer program was used to determine the main and secondary radiator masses. Figure 3.1.1 shows the masses of the different components of the platform along with the total platform mass as a function of maximum-allowable payload operating temperature. (The abbreviations used for the figure legend are: MR - main radiator, SR - secondary radiator, BOP - balance of platform, and TOT - total platform mass.) This figure shows that the mass of the secondary radiator decreases significantly as the payload temperature increases and that the secondary radiator mass is a large fraction of the total platform mass. Increasing the payload operating temperature from 400 K to 600 K results in a platform mass savings of about 39,000 kg, which is a decrease of 40%. A 30% decrease can be achieved by increasing the maximum-allowed payload temperature from 400 K to 500 K. Thus, even small improvements in the high-temperature capability of the payload electrical equipment afford significant platform mass savings.

In the base case, the separation distance between the main and secondary radiators was assumed to be 250 m. Varying this

separation distance provides an indication of the effect on the platform mass of radiant interaction between the two radiators. Figure 3.1.2 shows the platform mass as a function of separation distance for a payload operating at 440 K. More interaction between the radiators results in significantly greater secondary radiator and platform masses. The separation distance of 250 m was selected as an optimistic value for the base case because the radiator interaction is small at this distance. Smaller separation distances result in a secondary radiator mass that is a larger fraction of the total platform mass. Therefore, even larger mass savings would be achieved from the development of high-temperature electrical equipment.

For the base case, a 10 MWe platform was assumed. Platform mass calculations were also performed for 1 MWe and 0.1 MWe platforms to demonstrate that even lower power platforms will benefit from high temperature equipment, although to a lesser extent. Table 3.1.2 shows the results of the systems program for the 1 MWe and 0.1 MWe platforms.

Table 3.1.2

Brayton Cycle Systems Program Results (1 MWe & 0.1 MWe)

| | 1 MWe | 0.1 MWe |
|---|---|---|
| Thermal Power | 6.8 MW | 0.586 MW |
| Main Radiator Inlet Temperature | 816 K | 669 K |
| Main Radiator Outlet Temperature | 329 K | 277 K |
| Reactor Mass | 2591 kg | 2494 kg |
| Shield Mass | 1611 kg | 0 kg |
| Power Conversion System Mass | 658 kg | 74 kg |
| Miscellaneous Mass | 1346 kg | 422 kg |
| Total BOP Mass | 6205 kg | 2990 kg |

Figures 3.1.3 and 3.1.4 show the platform mass as a function of payload temperature for the 1 MWe and 0.1 MWe cases, respectively. Compared to the 10 MWe base case, the secondary radiator mass for the 1 MWe case is a smaller fraction of the total platform mass. However, it is still a large enough fraction that reductions in the secondary radiator mass have a significant effect on the total platform mass. For the 1 MWe case, increasing the payload temperature from 400 K to 600 K results in a 3,000 kg mass savings, or approximately a 17% reduction. For the 0.1 MWe case, the secondary radiator mass is a relatively small fraction of the total platform mass and so the benefits of increasing the payload temperature are not as pronounced. Increasing the payload operating temperature from 400 K to 600 K results in a 340 kg mass savings, which is only a 7% decrease.

Figure 3.1.5 shows the specific mass as a function of payload temperature for the 10 MWe, 1 MWe, and 0.1 MWe platforms. Specific mass is defined as the platform mass divided by the platform electric power. This figure shows that the platforms with smaller electric powers have higher specific masses and are thus less "mass efficient." However, the specific mass decreases as payload temperature increases regardless of the platform electric power. Figure 3.1.6 summarizes the relative mass savings achieved by increasing the payload temperature from 400 K to 600 K for the three different sized platforms. Platforms with the largest electric power demands offer the largest relative mass savings.

For the base case, 99% of the electric power consumed by the payload was assumed to degrade to waste heat. This is a reasonable assumption for most electrical equipment. However, for a radar, an appreciable fraction of the electric power may be removed from the payload by electromagnetic radiation in the radio wavelength band. To investigate this possibility, the base case was repeated with the assumption that only 50% of the payload electric power was converted to waste heat. The specific power as a function of payload temperature for this case is compared to the base case in Figure 3.1.7. With only 50% of the electric power converted to waste heat, the secondary radiator does not have to be as large; therefore, lower specific masses result. However, increasing the payload temperature from 400 K to 600 K still offers a 20,000 kg or 26% mass reduction for a 10 MWe platform.

As a final parametric case, the base case was repeated with two input changes. First, the temperature of space was increased from 250 K to 300 K; and second, the radiator mass per unit area values were increased by a factor of two. The higher space temperature is more representative of a high polar orbit. The larger radiator mass per area values are more representative of current state-of-the-art armored heat pipe radiators. This case is referred to as the realistic case. Figure 3.1.8 shows the platform masses as a function of payload temperature for this case. Because the secondary radiator mass is such a large fraction of the total platform mass, the savings realized by increasing payload temperature are much larger than for the base case. Increasing the payload temperature from 400 K to 600 K provides a 143,700 kg or 57% reduction in the platform mass.

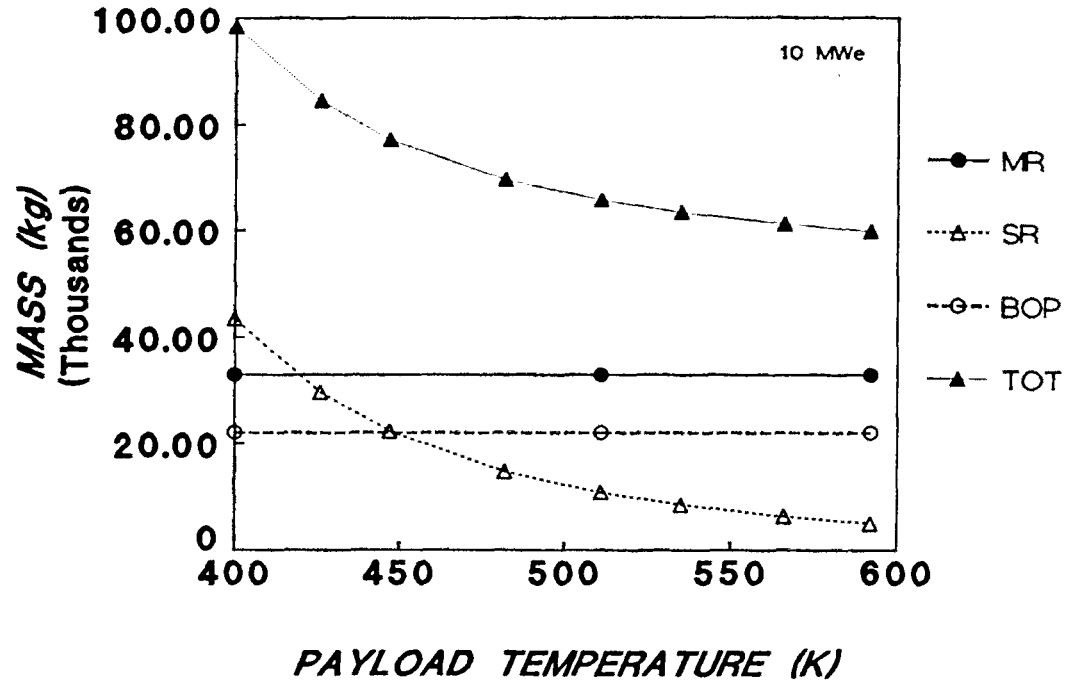


Figure 3.1.1 Base Case Platform Mass vs. Payload Temperature (Brayton Cycle Platform)

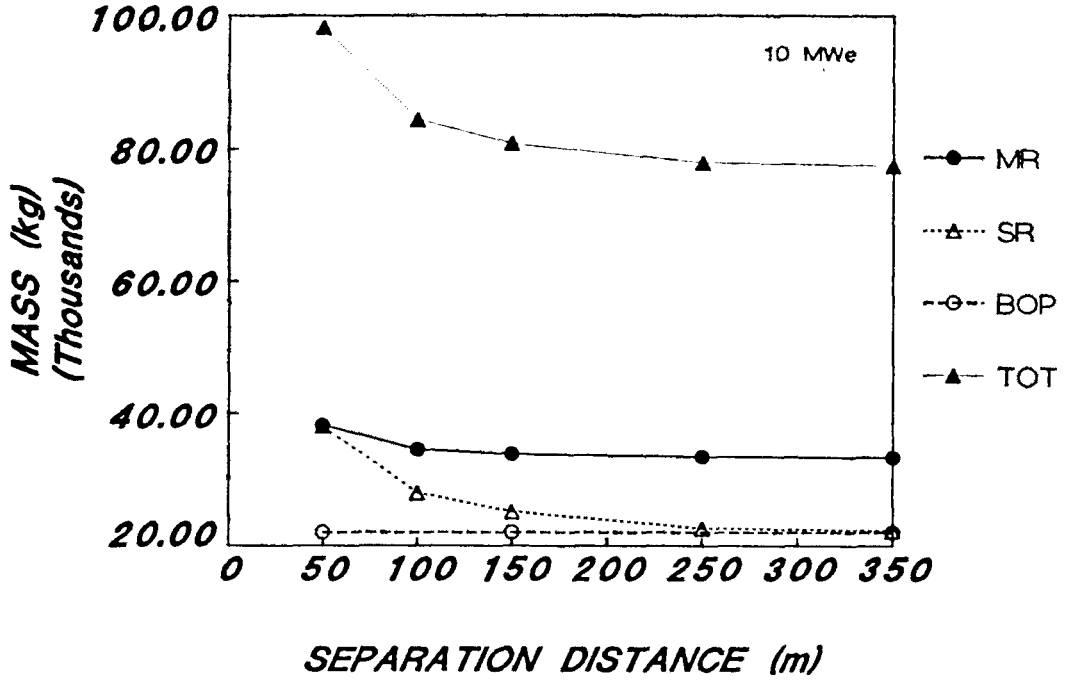


Figure 3.1.2 Base Case Platform Mass vs. Separation Distance (Brayton Cycle Platform)

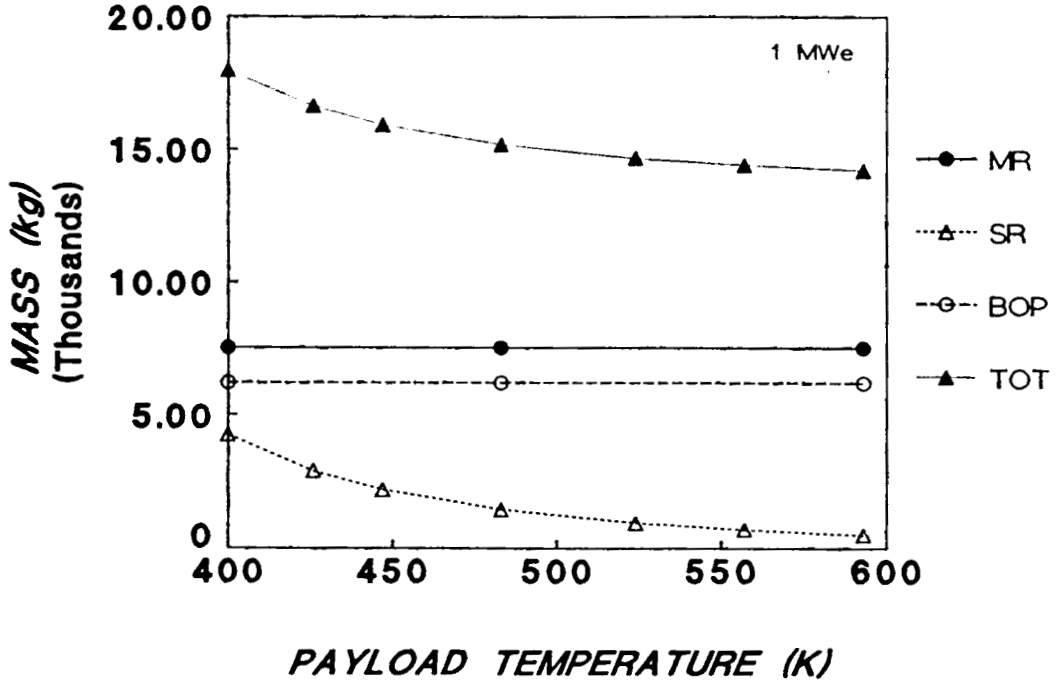


Figure 3.1.3 1 MWe Platform Mass vs. Payload Temperature
(Brayton Cycle Platform)

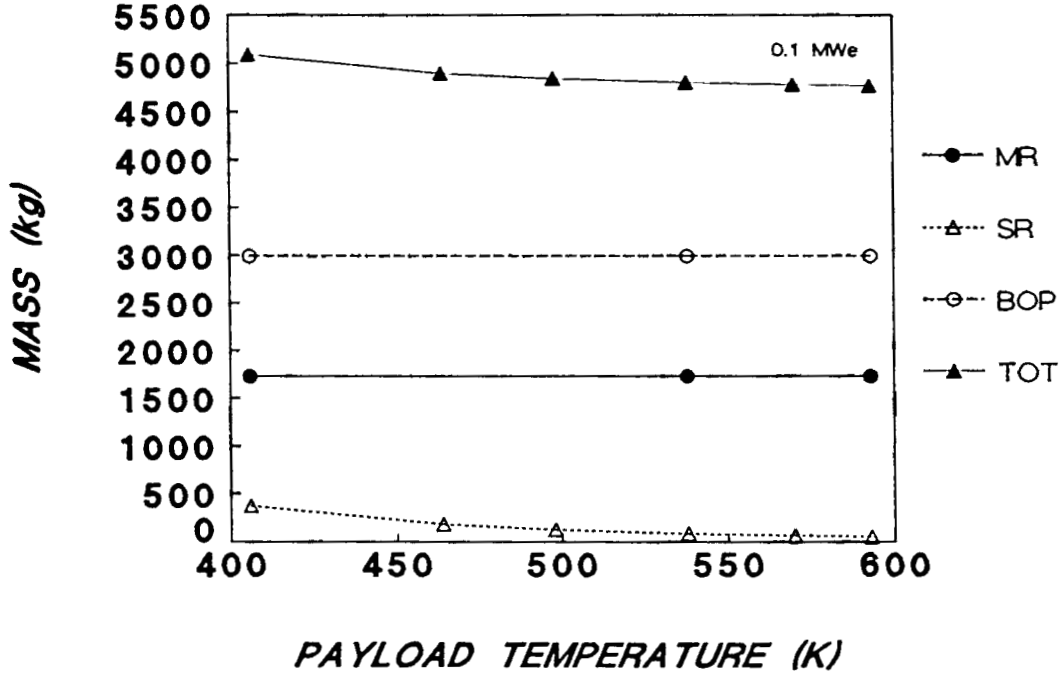


Figure 3.1.4 0.1 MWe Platform Mass vs. Payload Temperature
(Brayton Cycle Platform)

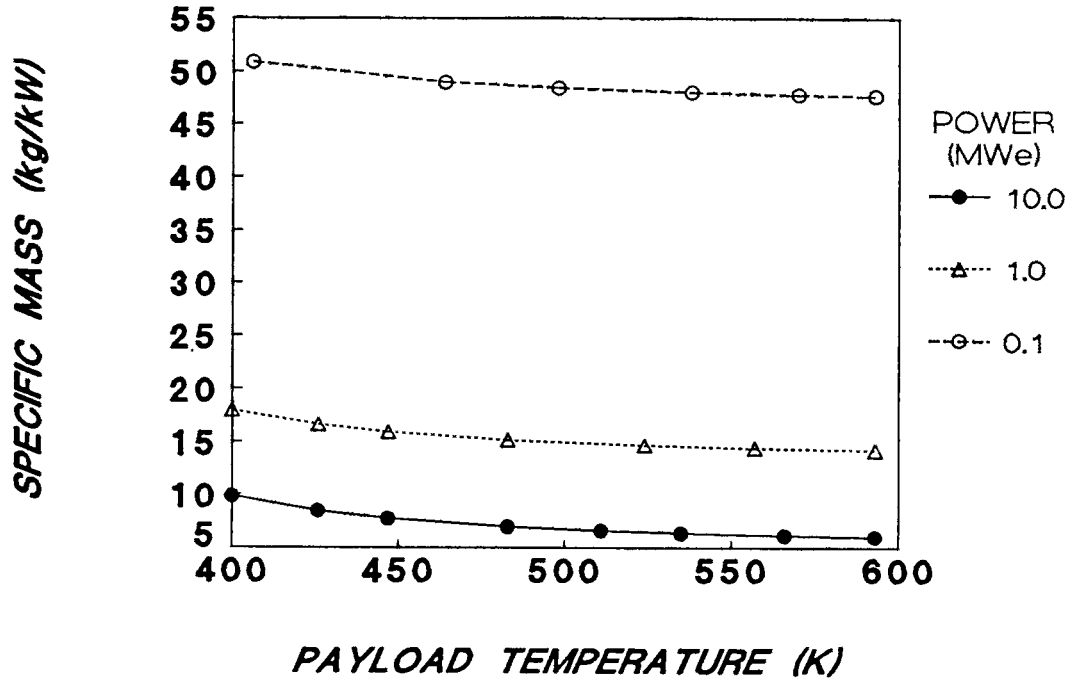


Figure 3.1.5 Platform Specific Mass vs. Payload Temperature for 10 MWe, 1 MWe, and 0.1 MWe Platforms (Brayton Cycle Platform)

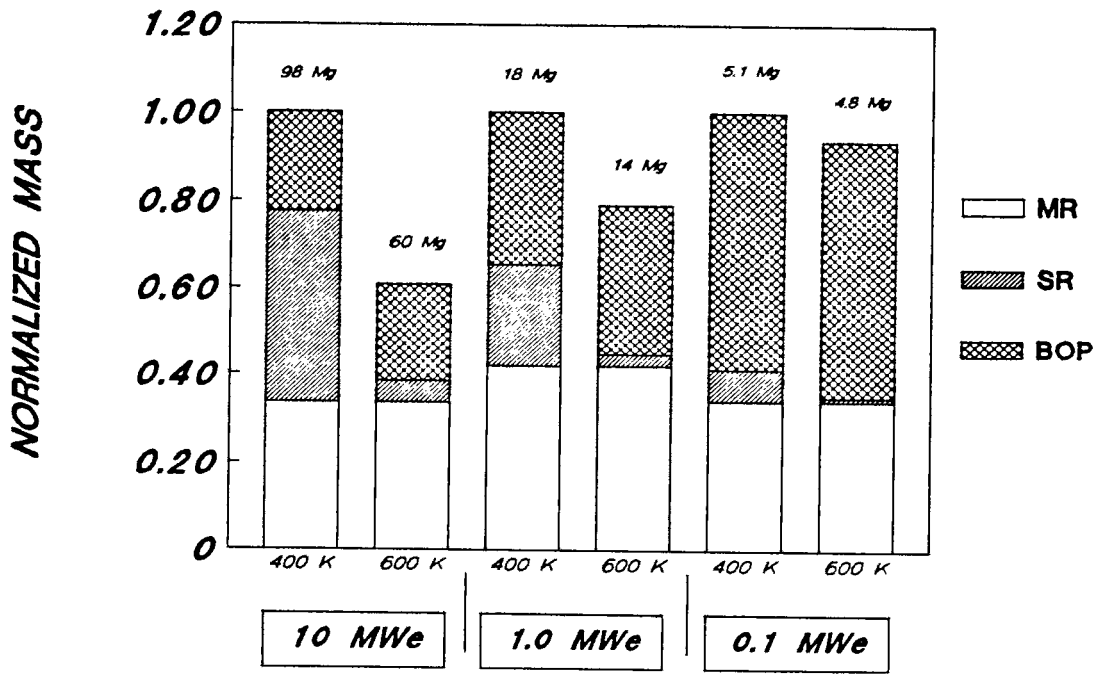


Figure 3.1.6 Summary of Platform Relative Mass Savings (Brayton Cycle Platform)

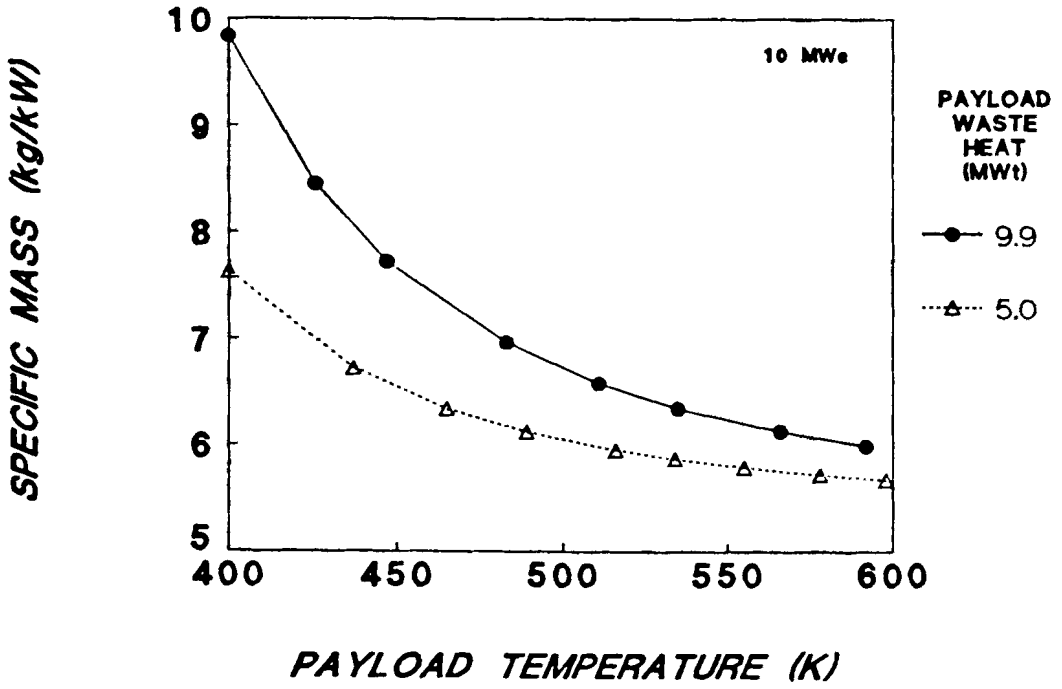


Figure 3.1.7 Platform Specific Mass vs. Payload Temperature for 9.9 MWt and 5.0 MWt of Payload Waste Heat (Brayton Cycle Platform)

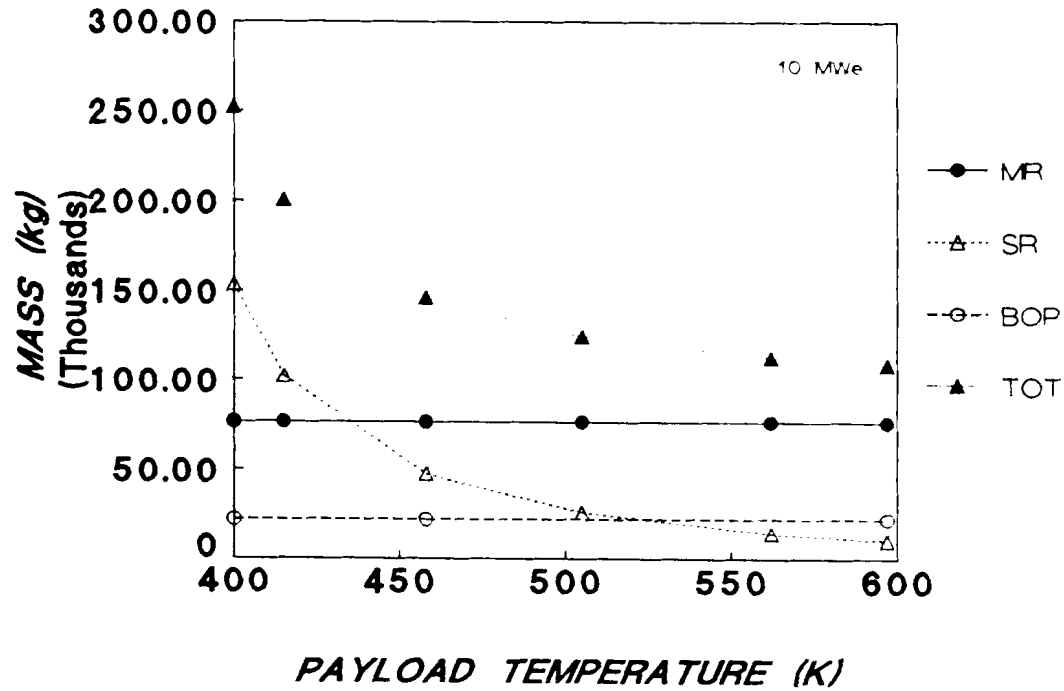


Figure 3.1.8 Realistic Case Platform Mass vs. Payload Temperature (Brayton Cycle Platform)

## 3.2 Payload Refrigerator

Platform mass calculations were also performed for the case in which a refrigerator was used to cool the payload. The possible advantage of using a refrigerator is that it allows the heat rejection temperature of the secondary radiator to be greater than the payload. Higher radiator temperatures allow a significant decrease in the secondary radiator mass, which is a large fraction of the total platform mass. The possible disadvantage of a refrigerator is that additional reactor power is required; this in turn leads to larger BOP and main radiator masses. The increase in mass associated with the refrigerator power demands must be less than the decrease in secondary radiator mass in order for a mass benefit to be realized. Even if a refrigerator does not result in a mass benefit compared to the pumped-loop payload cooling system, the use of high temperature electrical equipment in the payload offers overall platform mass savings. These savings occur because a higher payload temperature allows payload heat removal to the refrigerator working fluid at a higher temperature. This in turn increases the refrigerator COP, thus reducing the required additional power needed to run the refrigerator.

Figure 3.2.1 shows the platform masses as a function of the secondary radiator rejection temperature. These calculations were performed for a payload temperature of 450 K. Calculations were not performed for a secondary radiator temperature below 450 K because there is no need for a refrigerator in this case. As the figure shows, a higher rejection temperature results in a smaller secondary radiator mass; however, the masses of the BOP and main radiator increase as rejection temperature increases such that the overall platform mass also increases. Figure 3.2.2 compares the platform masses for the base case with and without a refrigerator for a payload temperature of 450 K. Two refrigerator cases are shown with different secondary radiator rejection temperatures, 500 K and 600 K. (The abbreviation REF is used to refer to the refrigerator in this figure.) This figure demonstrates the decrease in secondary radiator mass that occurs along with the increase in the BOP and main radiator masses. The net result is that for a Brayton cycle platform with a payload temperature of 450 K, the use of a refrigerator does not offer any mass benefit.

Figure 3.2.3 shows the total platform mass as a function of payload temperature for the base case with and without a refrigerator. A 500 K secondary radiator temperature was used for the with-refrigerator case. For payload temperatures below about 410 K, use of a refrigerator to cool the payload offers a small mass advantage. For payload temperatures greater than 410 K, the pumped-loop cooling system is slightly advantageous. What is clear from this figure is that higher payload temperatures result in significantly less massive platforms with either payload cooling system.

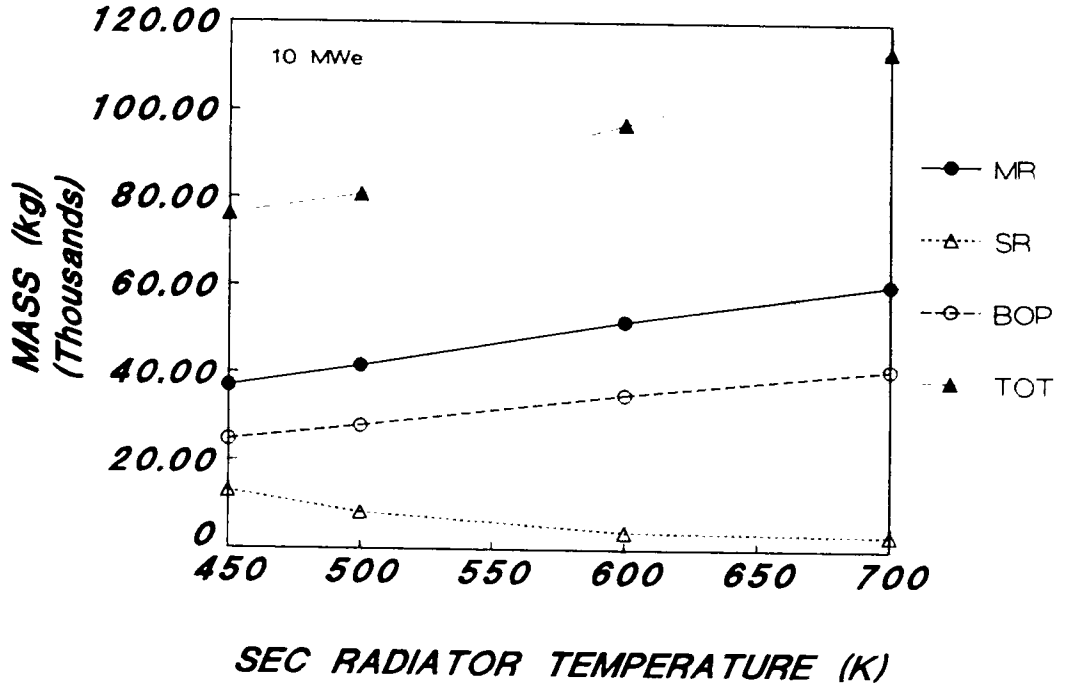


Figure 3.2.1 Platform Mass vs. Secondary Radiator Temperature (Brayton Cycle Platform)

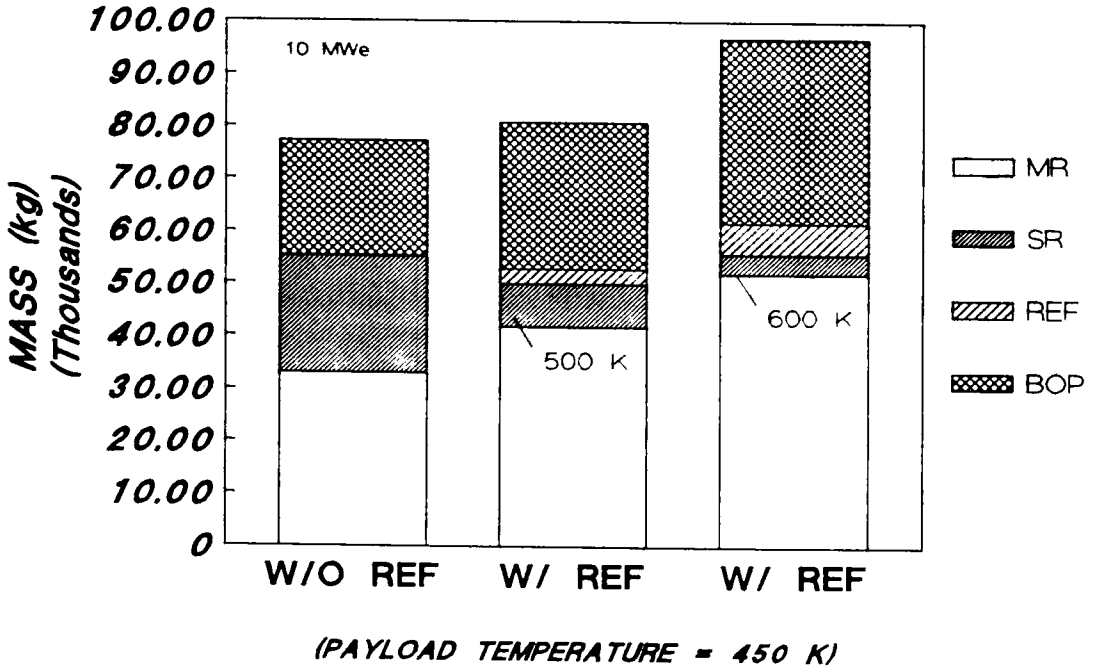


Figure 3.2.2 Base Case Platform Mass Comparison With and Without a Payload Refrigerator (Brayton Cycle Platform)

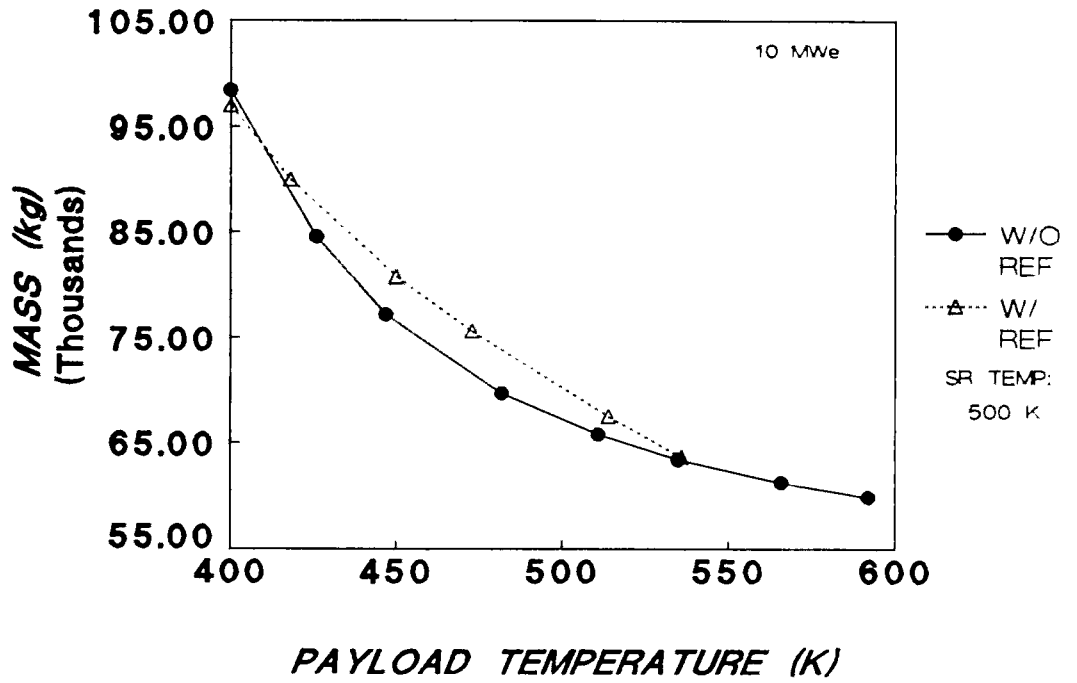


Figure 3.2.3 Platform Mass vs. Payload Temperature With and Without a Refrigerator (Brayton Cycle Platform)

# 4.0 RANKINE CYCLE PLATFORM RESULTS

## 4.1 Pumped-Loop Payload Cooling System

The same platform mass calculations performed for the Brayton cycle platform were repeated for a Rankine cycle platform. The major difference between the two platforms with respect to mass is that the Rankine cycle main radiator is relatively small compared to the Brayton cycle main radiator because heat is rejected at a higher temperature. Also, the liquid-metal cooled reactor of the Rankine cycle is much lighter than the gas-cooled Brayton cycle reactor. Therefore, the mass of the secondary radiator for the Rankine cycle platform accounts for a larger fraction of the total platform mass. Reductions in the secondary radiator mass thus are more pronounced with respect to the percentage of the platform mass.

Table 4.1.1 lists the systems program results for a 10 MWe Rankine cycle platform.

Table 4.1.1

Rankine Cycle Systems Program Results (Base Case)

| | |
|---|---|
| Thermal Power | 47 MW |
| Main Radiator Inlet Temperature | 820 K |
| Main Radiator Outlet Temperature | 820 K |
| Reactor Mass | 886 kg |
| Shield Mass | 1668 kg |
| Power Conversion System Mass | 9083 kg |
| Miscellaneous Mass | 1972 kg |
| Total BOP Mass | 13610 kg |

The platform heat transfer program was used next to determine the masses of the main and secondary radiators. Figure 4.1.1 shows the platform mass as a function of payload temperature for the base case. For a payload temperature of 400 K, the secondary radiator accounts for well over half of the total platform mass. Increasing the payload temperature to 600 K results in a 39,000 kg mass savings, which is a 61% reduction.

The effect of changing the separation distance between the two radiators is shown in Figure 4.1.2. As with the Brayton cycle platform, increasing the degree of radiant interaction between the two radiators (by decreasing the separation distance) greatly increases the platform mass. An optimistic separation distance of 250 m was selected for the base case,

assuming that the platform can be designed such that there is essentially no radiant interaction between the two radiators.

Mass calculations were also performed for a 1 MWe and a 0.1 MWe Rankine cycle platform. The results of the systems program are summarized in Table 4.1.2 for these two cases.

Table 4.1.2

Rankine Cycle Systems Program Results (1 MWe & 0.1 MWe)

| | 1 MWe | 0.1 MWe |
|---|---|---|
| Thermal Power | 4.74 MW | 0.417 MW |
| Main Radiator Inlet Temperature | 820 K | 770 K |
| Main Radiator Outlet Temperature | 820 K | 770 K |
| Reactor Mass | 311 kg | 303 kg |
| Shield Mass | 565 kg | 214 kg |
| Power Conversion System Mass | 1173 kg | 63 kg |
| Miscellaneous Mass | 286 kg | 67 kg |
| Total BOP Mass | 2335 kg | 647 kg |

The platform mass results for these two cases are shown in Figures 4.1.3 and 4.1.4. Although the BOP mass represents the predominate contributor to platform mass, the secondary radiator accounts for a relatively large part of the total mass. Therefore, decreases in the secondary radiator mass provide substantial platform mass savings, even for the 0.1 MWe case. Increasing the payload temperature from 400 K to 600 K results in a 52% (3,700 kg) mass reduction for the 1 MWe case and a 30% (330 kg) mass reduction for the 0.1 MWe case. Specific power as a function of payload temperature is provided in Figure 4.1.5 for the 10 MWe, 1 MWe, and 0.1 MWe cases. Figure 4.1.6 summarizes the relative mass savings for each of the three different sized platforms. As demonstrated by this figure, even the 0.1 MWe Rankine cycle platform realizes significant savings by increasing the allowable payload temperature.

The 10 MWe base case was repeated with the assumption that only 50% of the payload electric power is converted to waste heat. The platform specific mass for this case is compared to the base case in Figure 4.1.7. Although the mass savings are not as large as they are for the base case, significant mass savings can still be gained by increasing the maximum-allowed payload temperature.

As was done for the Brayton cycle platform, a parametric case for the Rankine cycle platform was performed with two

changes to the base case assumptions; namely, the temperature of space was increased from 250 K to 300 K and the radiator mass per unit area values were increased by a factor of two. The benefit of increasing payload temperatures is very large for this case as shown in Figure 4.1.8. Increasing the payload temperature from 400 K to 600 K allows a 134,250 kg or 78% decrease in platform mass. This overwhelming mass decrease results because the secondary radiator mass strongly dominates the platform mass.

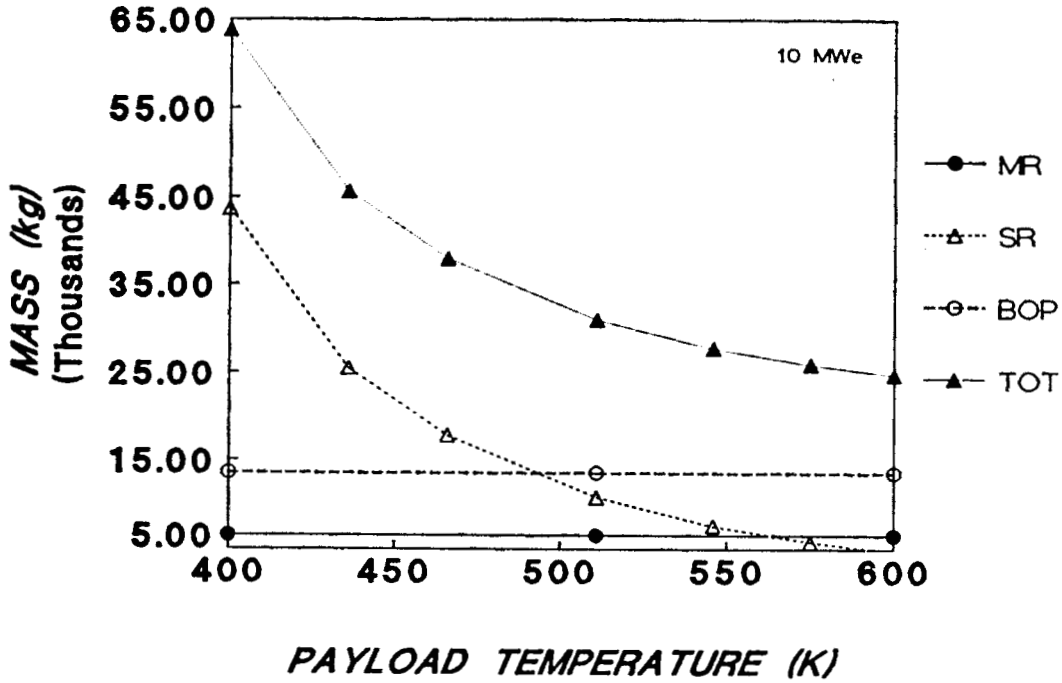


Figure 4.1.1 Base Case Platform Mass vs. Payload Temperature (Rankine Cycle Platform)

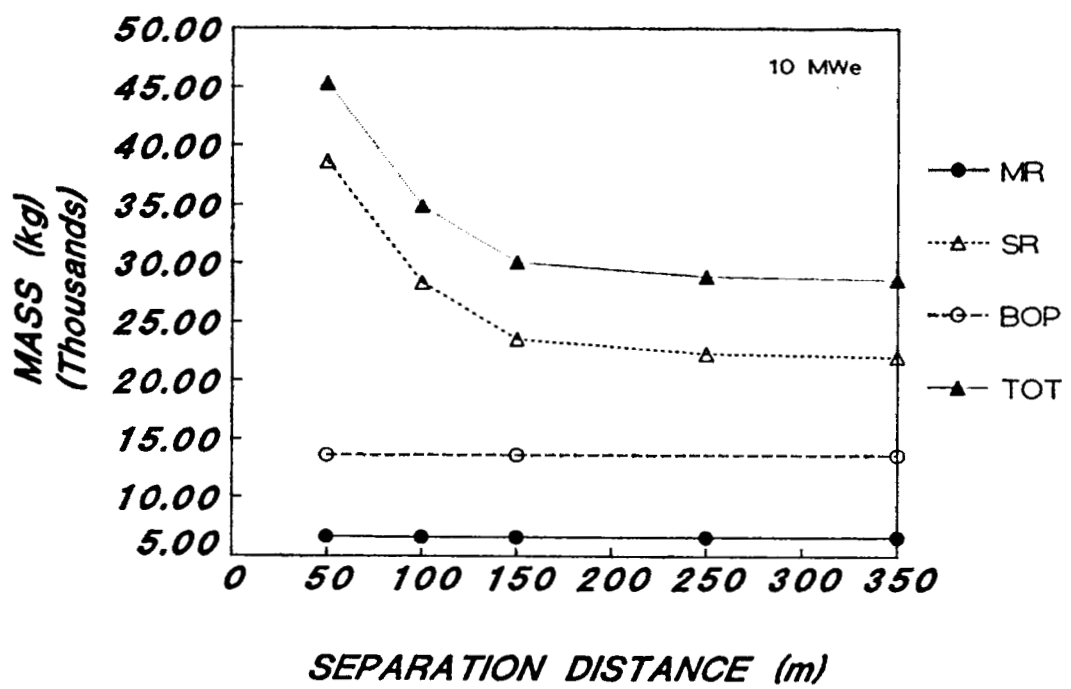


Figure 4.1.2 Base Case Platform Mass vs. Separation Distance (Rankine Cycle Platform)

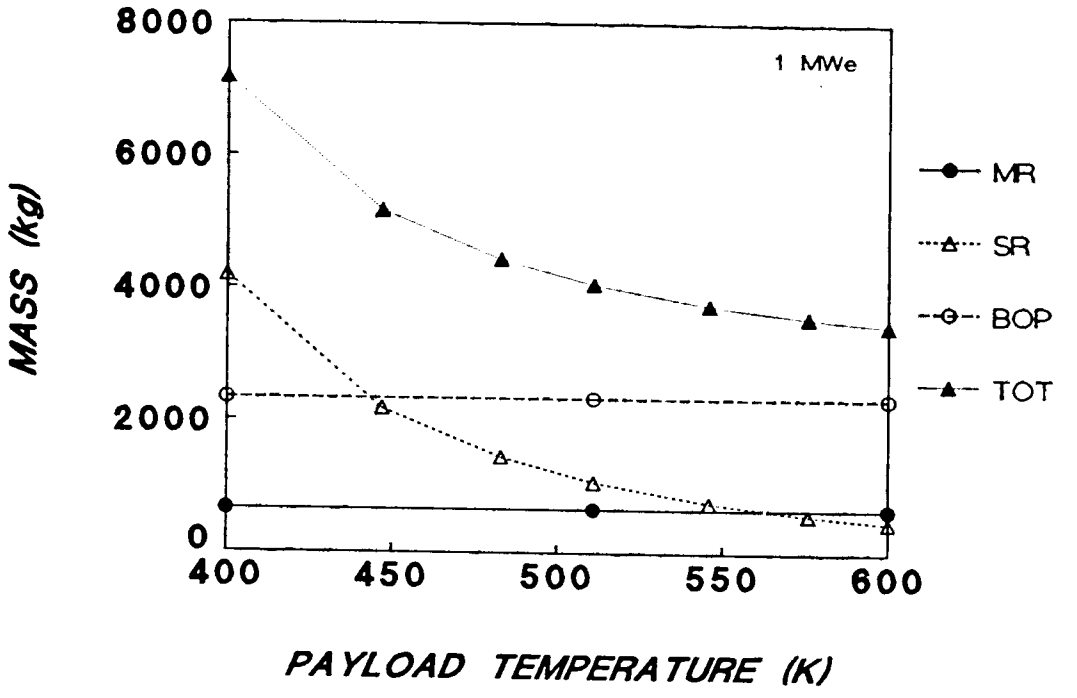


Figure 4.1.3 1 MWe Platform Mass vs. Payload Temperature (Rankine Cycle Platform)

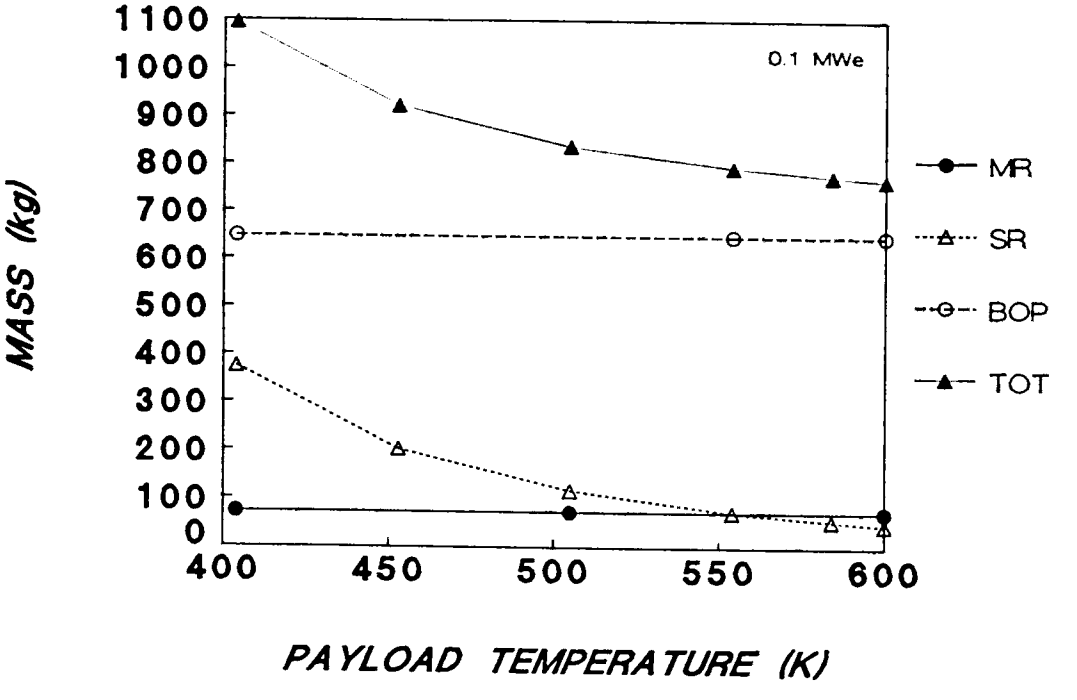


Figure 4.1.4 0.1 MWe Platform Mass vs. Payload Temperature (Rankine Cycle Platform)

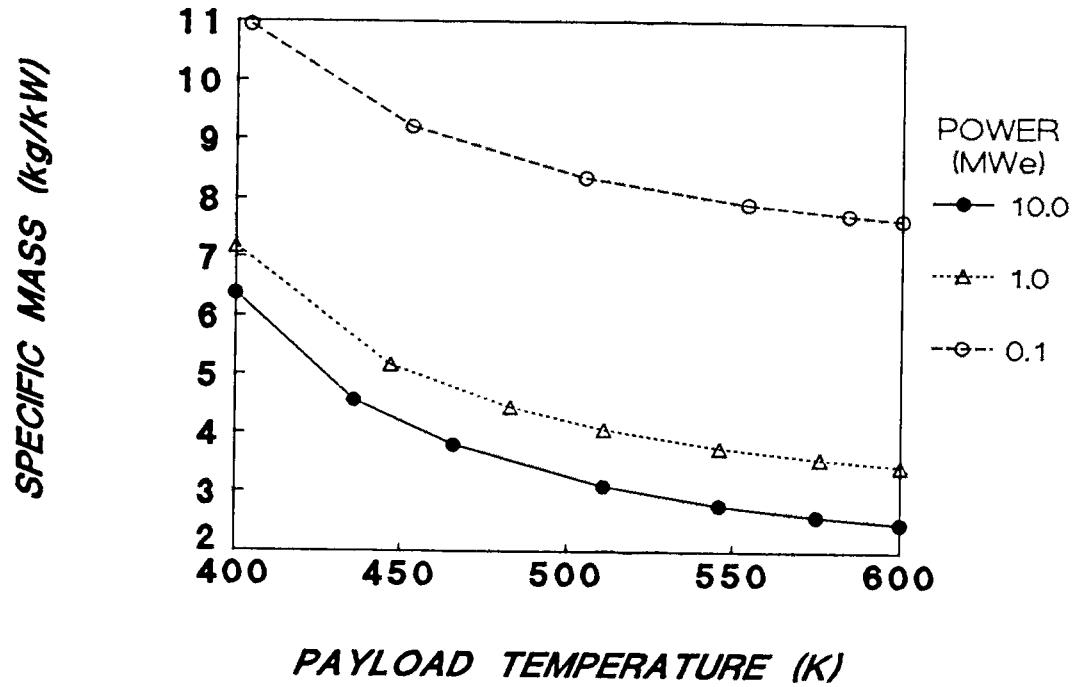


Figure 4.1.5 Platform Specific Mass vs. Payload Temperature for 10 MWe, 1 MWe, and 0.1 MWe Platforms (Rankine Cycle Platform)

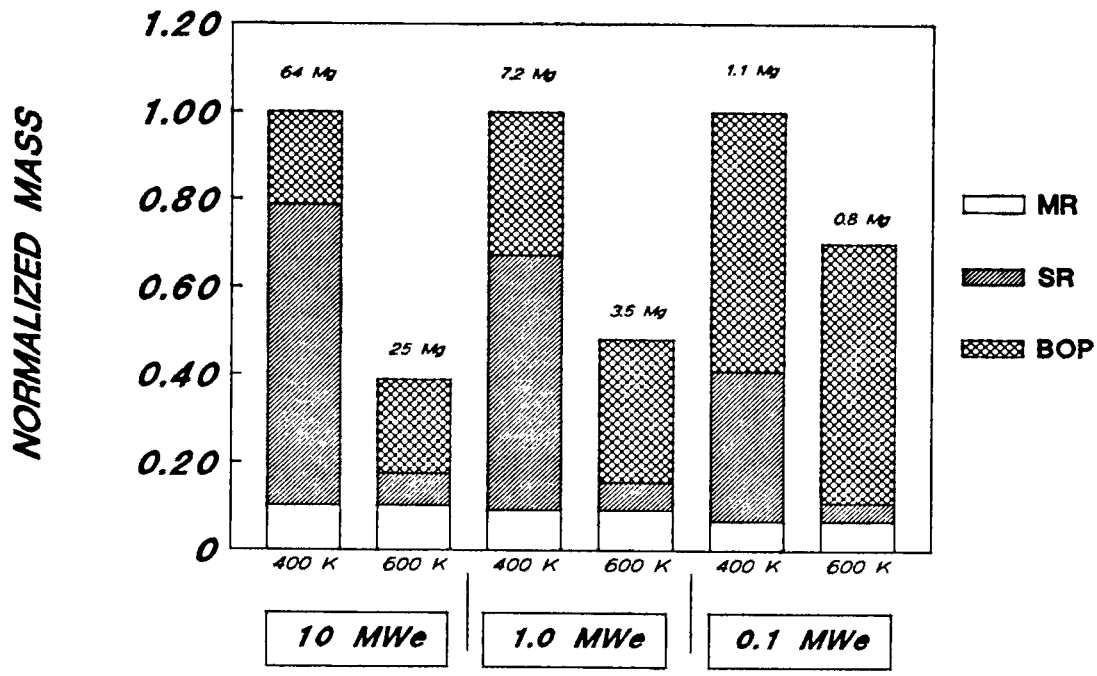


Figure 4.1.6 Summary of Relative Platform Mass Savings (Rankine Cycle Platform)

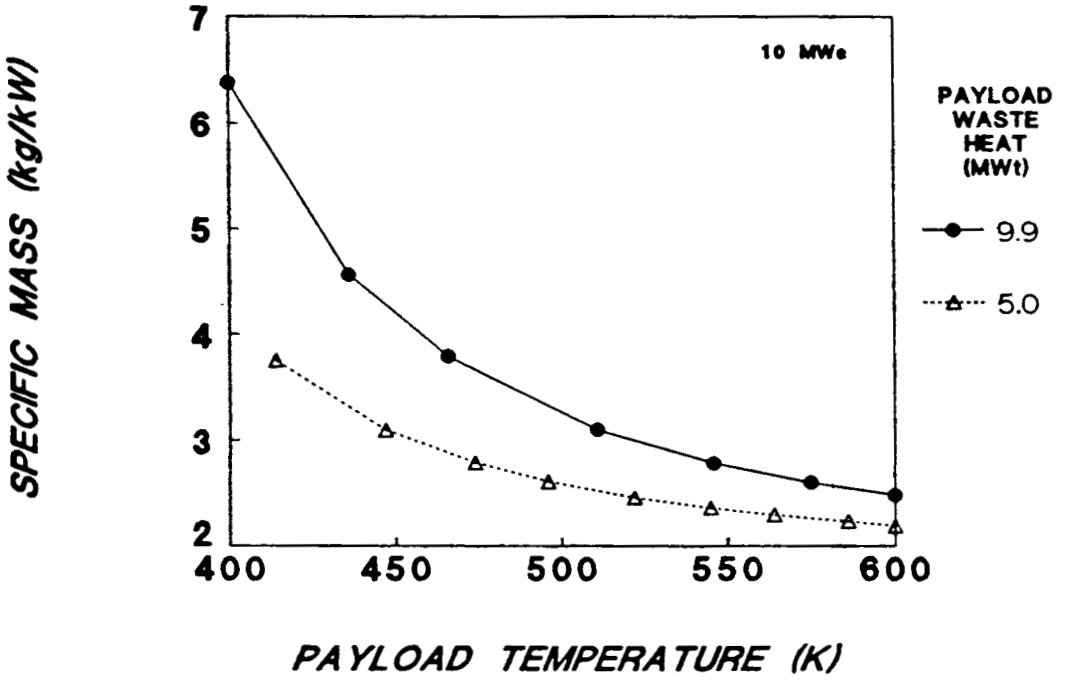


Figure 4.1.7 Platform Specific Mass vs. Payload Temperature for 9.9 MWt and 5.0 MWt of Payload Waste Heat (Rankine Cycle Platform)

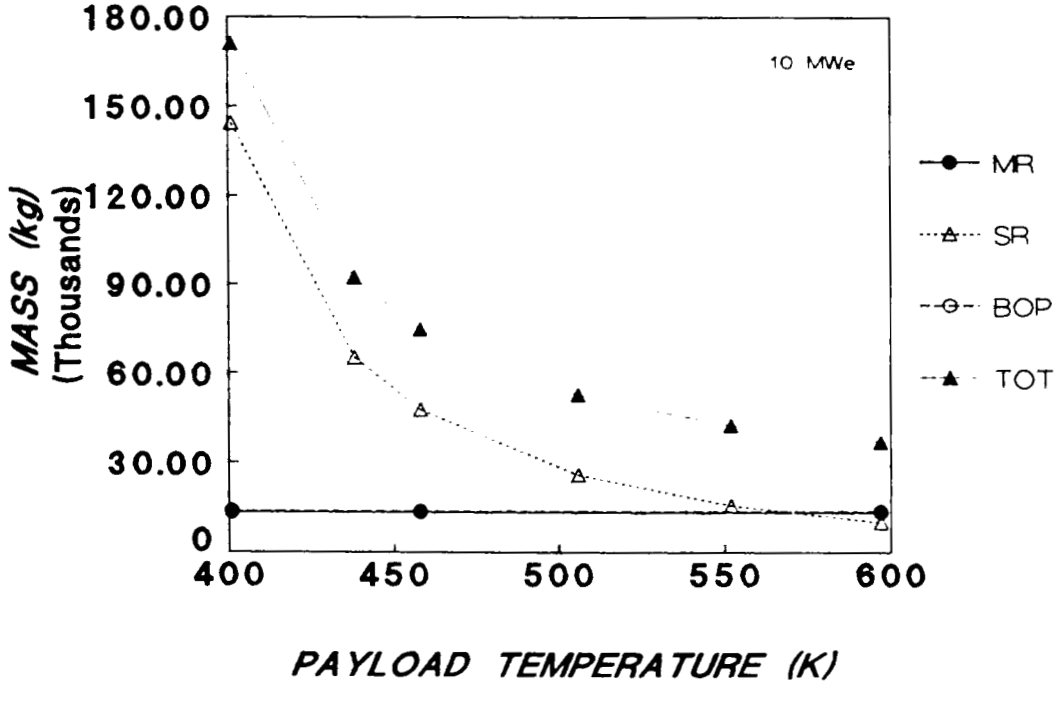


Figure 4.1.8 Realistic Case Platform Mass vs. Payload Temperature (Rankine Cycle Platform)

## 4.2 Payload Refrigerator

The use of a refrigerator to cool the payload was also investigated for a Rankine cycle platform. As with the Brayton cycle platform, increasing the waste heat rejection temperature decreases the mass of the secondary radiator but increases the mass of the BOP and main radiator. Figure 4.2.1 shows that a minimum platform mass occurs at a secondary radiator temperature of about 500 K. Any further increase in rejection temperature lowers the secondary radiator mass but increases the total platform mass.

Figure 4.2.2 compares the platform mass results for the base case with and without a refrigerator. The with-refrigerator cases are shown for secondary radiator temperatures of 500 K (the optimum rejection temperature) and 600 K. This figure shows that the use of a refrigerator to cool the payload for a Rankine cycle can result in about a 10% decrease in the platform mass compared to the without-refrigerator case. These results are for a payload temperature of 450 K. Figure 4.2.3 shows that the mass savings offered by a refrigerator diminish as the payload temperature increases. Another way to view this is to say that a platform using a pumped-loop heat exchanger to cool the payload with a 450 K payload temperature has about the same mass as a platform using a refrigertor-cooled payload at 400 K. Thus, higher payload temperatures allow the reduction of the platform mass without the added complexity of a refrigerator. A final point to be made about this figure is that with or without a refrigerator, higher payload temperatures result in lower platform masses.

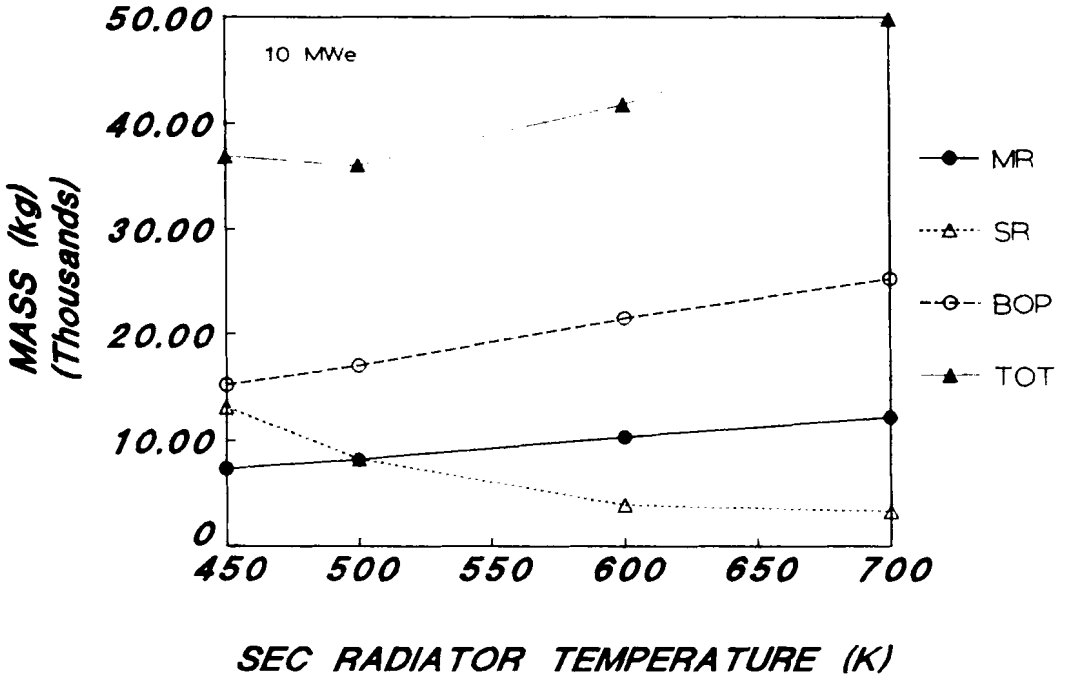


Figure 4.2.1 Platform Mass vs. Secondary Radiator Temperature (Rankine Cycle Platform)

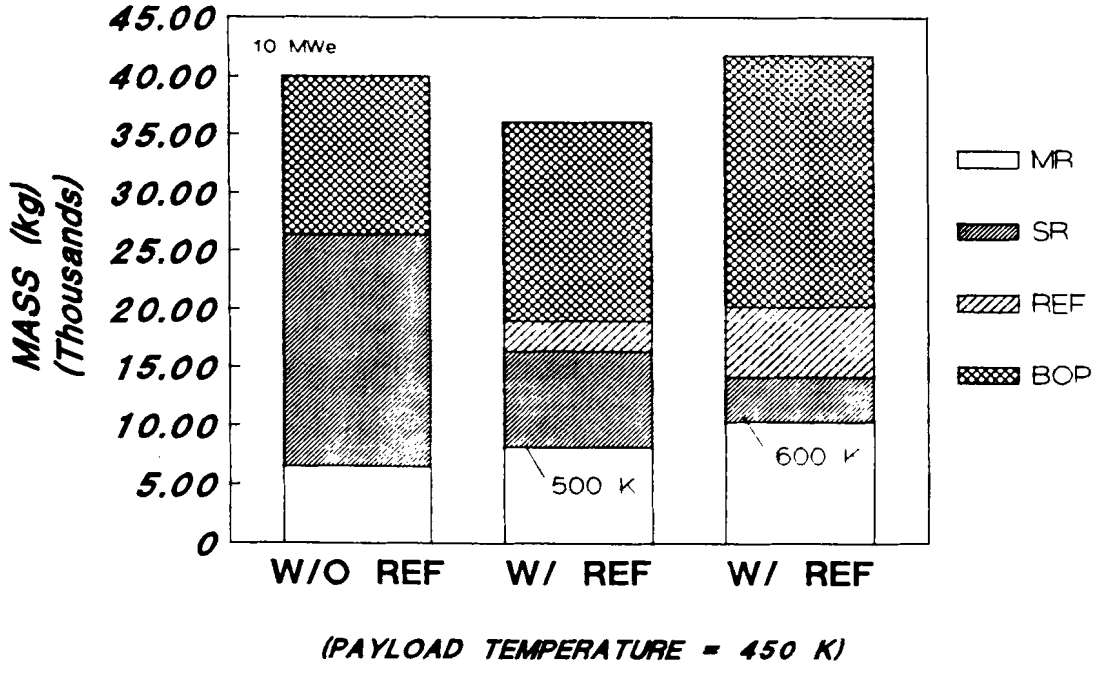


Figure 4.2.2 Base Case Platform Mass Comparison With and Without a Payload Refrigerator (Rankine Cycle Platform)

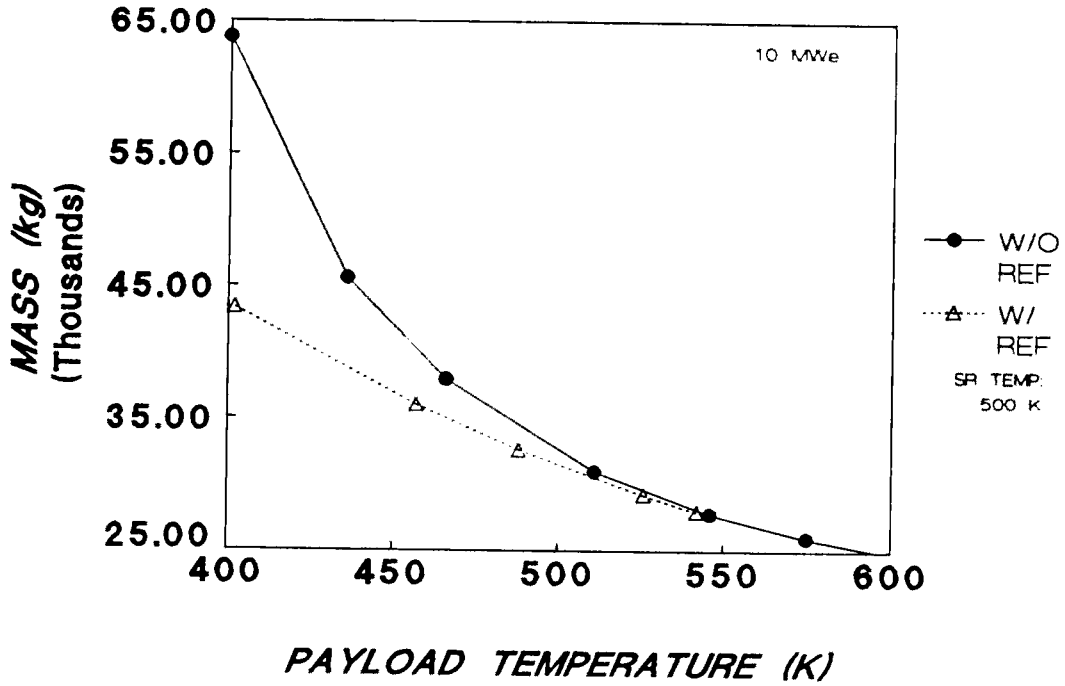


Figure 4.2.3 Platform Mass vs. Payload Temperature With and Without a Refrigerator (Rankine Cycle Platform)

## 5.0 SUMMARY AND CONCLUSIONS

Calculations were performed to determine the mass of a space-based platform as a function of the maximum-allowed payload operating temperature. Two computer programs were used in conjunction to perform these calculations. The first program was used to determine the mass of the platform reactor, shield, and power conversion system. The second program was used to determine the mass of the main and secondary radiators of the platform. The main radiator removes the waste heat associated with the power conversion system and the secondary radiator removes the waste heat associated with the platform payload. These calculations were performed for both Brayton and Rankine cycle platforms with two different types of payload cooling systems: a pumped-loop system using a heat exchanger with a liquid working fluid and a refrigerator system.

The results indicate that with either type of payload cooling, higher payload temperatures result in overall platform mass savings for both kinds of platforms. For the pumped-loop cases, these mass savings occur because higher payload temperatures allow a reduction in the amount of waste heat to be rejected actively and because the payload waste heat can be rejected by the secondary radiator at higher temperatures. This second advantage can be very large because of the fourth power dependence of temperature on radiator area. For the refrigerator cases, the mass savings occur because of the reduction in the amount of waste heat to be rejected actively and because higher payload temperatures result in higher refrigerator COPs. More efficient refrigerators decrease the power demands of the refrigerator resulting in reduced BOP and main radiator masses.

With the pumped-loop cooled payloads, the relative mass savings for the Rankine cycle platforms are greater than for the Brayton cycle platform because the secondary radiator accounts for a larger fraction of the total platform mass. Thus, reductions in the mass of the secondary radiator, for the Rankine cycle platform, represent a larger fractional reduction of the total platform mass. With the refrigerator-cooled payloads, the relative mass savings are about the same for the two kinds of platforms.

The results also indicate that significant mass savings can be achieved even for modest increases in the high temperature capability of the payload. When reviewing these results, one should keep in mind that optimistic values of the input variables were selected for these analyses; more realistic values lead to greater mass savings and make high temperature electrical components even more attractive.

The analyses presented in this document were performed primarily to demonstrate the dependence of platform mass on the maximum-allowed payload temperature. Based on these analyses, three additional and important comments are in order.

(1) The secondary radiator mass can account for a large fraction of the total platform mass and must be included in any platform mass estimates.

(2) The size of both the main and secondary radiators is strongly dependent on their relative proximity to each other and to other platform structures. This dependence should be considered when sizing space platform radiators.

(3) Cooling the payload with a refrigerator essentially eliminates the mass penalty associated with the secondary radiator; however, when a refrigerator is used, the mass penalty associated with the BOP and main radiator can be very significant and may negate the advantage of decreasing the secondary radiator mass. (Also, reliability issues associated with the use of very large refrigerators are not addressed in this report but should be considered when deciding on their use.)

Reiterating, the overall conclusion of this report is that increases in the high temperature capability of the payload electrical equipment offer significant platform mass savings. This is true for both Brayton and Rankine cycle platforms with pumped-loop or refrigerator cooled payloads.

## 6.0 REFERENCES

1. Michael W. Edenburn, "Models for Multimegawatt Space Power Systems," SAND86-2742, (to be published).

2. Dean Dobranich, "Estimating Payload Internal Temperatures and Radiator Size for Multimegawatt Space Platforms," SAND87-1216, August, 1987.

3. Albert C. Marshall, "RSMASS: A Preliminary Reactor/Shield Mass Model for SDI Applications," SAND86-1020, August 1986.

DISTRIBUTION

AFAT/SAS
Fort Walton Beach, FL 32542
Attn: Capt. Jerry Brown

AFISC/SNAR
Kirtland Air Force Base
New Mexico 87117
Attn: Lt. Col. J. P. Joyce

AF Astronautics Laboratory/LKCJ
Edwards Air Force Base
California 93523
Attn: G. Beale

AF Astronautics Laboratory/LKCJ
Edwards Air Force Base
California 93523
Attn: F. Meade

AF Astronautics Laboratory/LKCJ
Edwards Air Force Base
California 93523
Attn: Lt. R. Henley

AF Astronautics Laboratory/LKCJ
Edwards Air Force Base
California 93523
Attn: Major E. Houston

AFWAL/AA
Wright-Patterson AFB
Ohio 45433
Attn: Dick Renski

AFWAL/POOS
Wright-Patterson AFB
Ohio 45433
Attn: E. B. Kennel

AFWAL/POOC-1
Bldg. 450
Wright-Patterson AF Base
Ohio 45433
Attn: R. Thibodeau

AFWAL/POO
Aeronautical Laboratory
Wright-Patterson AFB
Ohio 45433
Attn: W. Borger

AFWAL/POOA
Aeronautical Laboratory
Bldg. 18
Wright-Patterson AFB
Ohio 45433
Attn: P. Colegrove

AFWAL/POOC-1
Aeronautical Laboratory
Bldg. 450
Wright-Patterson AFB
Ohio 45433
Attn: D. Massie

AFWAL/POOC-1
Aeronautical Laboratory
Wright-Patterson AFB
Ohio 45433
Attn: C. Oberly

AFWAL/POOC-1
Aeronautical Laboratory
Wright-Patterson AFB
Ohio 45433
Attn: T. Mahefky

AFWAL/POOS
Wright-Patterson AFB
Ohio 45433
Attn: J. Beam

AFWAL/POOC-1
Power Components Branch
Wright Patterson AFB
Ohio 45433-6563

AFWAL/POOC
Aeronautical Laboratory
Bldg. 18
Wright-Patterson AFB
Ohio 45433
Attn: Major Seward

AFWL/AFSC
Kirtland Air Force Base
New Mexico 87117
Attn: M. J. Schuller

AFWL/AW
Kirtland AFB
New Mexico 87117
Attn: D. Kelleher

AFWL/AWYS
Kirtland Air Force Base
New Mexico 87117
Attn: Lt. Col. Jackson

AFWL/AWYS
Kirtland Air Force Base
New Mexico 87117
Attn: Major D. R. Boyle

HQ AFSPACECOM/XPXIS
Peterson Air Force Base
Colorado 80914-5001
Attn: Lt. Col. F. Lawrence

HQ USAF/RD-D
Washington, DC 20330-5042
Attn: Maj. P. Talty

Aerospace Corporation
P. O. Box 9113
Albuquerque, NM 87119
Attn: W. Zelinsky

Aerospace Corporation
P. O. Box 9113
Albuquerque, NM 87119
Attn: W. Blocker

Aerospace Corporation
P. O. Box 9113
Albuquerque, NM 87119
Attn: M. Firmin

Aerospace Corporation
P. O. Box 92957
El Segundo, CA 90009
Attn: P. Margolis

Air Force Center for Studies
and Analyses/SASD
The Pentagon, Room ID-431
Washington, DC 20330-5420
Attn: W. Barattino, AFCSA/SASD

Air Force Foreign Technology Div
TQTD
Wright-Patterson AFB
Ohio 45433-6563
Attn: B. L. Ballard

Air Force Foreign Technology Div.
TQTD
Wright-Patterson AFB
Ohio 45433-6563
Attn: K. W. Hoffman

Air Force Space Technology Center
SWL
Kirtland AFB, NM 87117-6008
Attn: Capt. M. Brasher

Air Force Space Technology Center
SWL
Kirtland AFB, NM 87117-6008
Attn: J. DiTucci

Air Force Space Technology Center
SWL
Kirtland AFB, NM 87117-6008
Attn: Capt. E. Fornoles

Air Force Space Technology Center
TP
Kirtland AFB, NM 87117-6008
Attn: M. Good

Air Force Space Technology Center
XLP
Kirtland AFB, NM 87117-6008
Attn: A. Huber

Air Force Space Technology Center
SWL
Kirtland AFB, NM 87117-6008
Attn: S. Peterson

ANSER Corp.
Crystal Gateway 3
1225 Jefferson Davis Highway #800
Arlington, VA 22208
Attn: K. C. Hartkay

Argonne National Laboratory
9700 S. Cass Avenue
Argonne, IL 60439
Attn: S. Bhattacharyya

Argonne National Laboratory
9700 S. Cass Avenue
Argonne, IL 60439
Attn: D. C. Fee

Argonne National Laboratory
9700 S. Cass Avenue
Argonne, IL 60439
Attn: K. D. Kuczen

Argonne National Laboratory
9700 S. Cass Avenue
Argonne, IL 60439
Attn: R. A. Lewis

Argonne National Laboratory
9700 S. Cass Avenue
Argonne, IL 60439
Attn: D. C. Wade

Auburn University
202 Sanform Hall
Auburn, AL 36849-3501
Attn: Dr. T. Hyder

Auburn University
231 Leach Center
Auburn, AL 36849-3501
Attn: F. Rose

Avco Research Laboratory
2385 Revere Beach Pkwy
Everett, MA 02149
Attn: D. W. Swallom

Babcock & Wilcox
Nuclear Power Division
3315 Old Forest Road
P.O. Box 10935
Lynchburg, VA 24506-0935
Attn: B. J. Short

Battelle Pacific Northwest Lab.
P. O. Box 999
Richland, WA 99352
Attn: J. O. Barner

Battelle Pacific Northwest Lab.
P. O. Box 999
Richland, WA 99352
Attn: L. Schmid

Battelle Pacific Northwest Lab.
P. O. Box 999
Richland, WA 99352
Attn: E. P. Coomes

Battelle Pacific Northwest Lab
Battelle Boulevard
Richland, WA 99352
Attn: B. M. Johnson

Battelle Pacific Northwest Lab.
P. O. Box 999
Richland, WA 99352
Attn: W. J. Krotiuk

Battelle Pacific Northwest Lab.
P. O. Box 999
Richland, WA 99352
Attn: R. D. Widrig

Boeing Company
P.O. Box 3999
MS 8K-30
Seattle, WA 98124-2499
Attn: A. Sutey

Boeing Company
Boeing Aerospace System
P.O. Box 3707
Seattle, WA 98124
Attn: K. Kennerud

Brookhaven National Laboratory
P.O. Box 155
Upton, NY 11973
Attn: T. Bowden

Brookhaven National Laboratory
P.O. Box 155
Upton, NY 11973
Attn: H. Ludewig

Brookhaven National Laboratory
P.O. Box 155
Upton, NY 11973
Attn: W. Y. Kato

Brookhaven National Laboratory
P.O. Box 155
Bldg. 701, Level 143
Upton, NY 11973
Attn: J. Powell

California Inst. of Technology
Jet Propulsion Laboratory
4800 Oak Grove Drive
Pasadena, CA 91109
Attn: V. C. Truscello

California Inst. of Technology
Jet Propulsion Laboratory
4800 Oak Grove Drive
Pasadena, CA 91109
Attn: P. Bankston

California Inst. of Technology
Jet Propulsion Laboratory
4800 Oak Grove Drive
Pasadena, CA 91109
Attn: E. P. Framan

California Inst. of Technology
Jet Propulsion Laboratory
4800 Oak Grove Drive
Pasadena, CA 91109
Attn: L. Isenberg

California Inst. of Technology
Jet Propulsion Laboratory
4800 Oak Grove Drive
Pasadena, CA 91109
Attn: J. Mondt

DARPA
1400 Wilson Blvd.
Arlington, VA 22209
Attn: P. Kemmey

DCSCON Consulting
4265 Drake Court
Livermore, CA 94550
Attn: D. C. Sewell

Defense Nuclear Agency
6801 Telegraph Road
Alexandria, VA 22310-3398
Attn: J. Farber/RAEV

DNA/RAEV
6801 Telegraph Road
Alexandria, VA 22310-3398
Attn: J. Foster

EG&G Idaho, Inc./INEL
P.O. Box 1625
Idaho Falls, ID 83415
Attn: R. Rice

EG&G Idaho, Inc./INEL
P.O. Box 1625
Idaho Falls, ID 83415
Attn: J. Dearien

EG&G Idaho, Inc./INEL
P.O. Box 1625
Idaho Falls, ID 83415
Attn: M. L. Stanley

EG&G Idaho, Inc./INEL
P.O. Box 1625
Idaho Falls, ID 83415
Attn: R. D. Struthers

EG&G Idaho, Inc./INEL
P.O. Box 1625
Idaho Falls, ID 83415
Attn: J. F. Whitbeck

EG&G Idaho, Inc./INEL
P.O. Box 1625
Idaho Falls, ID 83415
Attn: P. W. Dickson

EG&G Idaho, Inc./INEL
P.O. Box 1625
Idaho Falls, ID 83415
Attn: J. W. Henscheid

Ford Aerospace Corporation
Aeronutronic Div.
Ford Road, P.O. Box A
Newport Beach, CA 92658-9983
Attn: V. Pizzuro

GA Technologies
P.O. Box 85608
San Diego, CA 92138
Attn: H. J. Snyder

GA Technologies
P.O. Box 85608
San Diego, CA 92138
Attn: C. Fisher

GA Technologies
P.O. Box 85608
San Diego, CA 92138
Attn: R. Dahlberg

Garrett Fluid Systems Co.
P.O. Box 5217
Phoenix, AZ 85010
Attn: Robert Boyle

General Electric Company
P. O. Box 8555
Astro Systems
Philadelphia, PA 19101
Attn: R. J. Katucki

General Electric Corp/NSTO
310 DeGuigne Drive
Sunnyvale, CA 9048
Attn: C. Cowan

General Electric NSTO
310 DeGuigne Drive
Sunnyvale, CA 90486
Attn: E. E. Gerrels

General Electric NSTO
310 DeGuigne Drive
Sunnyvale, CA 90486
Attn: H. S. Bailey

General Electric-SCO
P. O. Box 8555
Astro Systems
Philadelphia, PA 19101
Attn: J. Chan

General Electric
P. O. Box 8555
Bldg. 100, Rm M2412
Astro Systems
Philadelphia, PA 19101
Attn: J. Hnat

General Electric
P. O. Box 8555
Astro Systems
Philadelphia, PA 19101
Attn: R. D. Casagrande

General Electric
P. O. Box 8555
Astro Systems
Philadelphia, PA 19101
Attn: W. Chiu

Grumman Aerospace Corporation
M/S B20-05
Bethpage, NY 11714
Attn: J. Belisle

Hanford Engineering Dev. Lab
Post Office Box 1970
Richland, WA 99352
Attn: D. S. Dutt

House of Representatives Staff
Space and Technology Committee
2320 Rayburn Building
Washington, DC 20515
Attn: Tom Weimer

Idaho National Engineering
Laboratory
P. O. Box 1625
Idaho Fall, ID 83414
Attn: W. H. Roack

Innovative Nuclear Space Pwr.Inst.
202 NSC
University of Florida
Gainesville, FL 32611
Attn: N. J. Diaz

International Energy Assoc. Ltd.
1717 Louisiana NE
Suite 202
Albuquerque, NM 87110
Attn: G. B. Varnado

Lawrence Livermore National Lab.
P. O. Box 808
Livermore, CA 94550
Attn: Lynn Cleland, MS L-144

Lawrence Livermore National Lab.
P. O. Box 808
Livermore, CA 94550
Attn: C. E. Walter, MS L-144

Los Alamos National Laboratory
P. O. Box 1663
Los Alamos, NM 87545
Attn: T. Trapp, MS-E561

Los Alamos National Laboratory
P. O. Box 1663
Los Alamos, NM 87545
Attn: R. Hardie, MS-F611

Los Alamos National Laboratory
P. O. Box 1663
Los Alamos, NM 87545
Attn: C. Bell, MS A145

Los Alamos National Laboratory
P. O. Box 1663
Los Alamos, NM 87545
Attn: R. J. LeClaire

Los Alamos National Laboratory
P. O. Box 1663
Los Alamos, NM 87545
Attn: S. Jackson, MS-F611

Los Alamos National Laboratory
P. O. Box 1663
Los Alamos, NM 87545
Attn: J. Metzger

Los Alamos National Laboratory
P. O. Box 1663
Los Alamos, NM 87545
Attn: C. W. Watson, MS-F607

Los Alamos National Laboratory
P. O. Box 1663
Los Alamos, NM 87545
Attn: Don Reid, MS-H811

Los Alamos National Laboratory
P. O. Box 1663
Los Alamos, NM 87545
Attn: R. Bohl, MS-K551

Los Alamos National Laboratory
P. O. Box 1663
Los Alamos, NM 87545
Attn: D. R. Bennett

Los Alamos National Laboratory
P. O. Box 1663
Los Alamos, NM 87545
Attn: W. L. Kirk

Los Alamos National Laboratory
P. O. Box 1663
Los Alamos, NM 87545
Attn: M. Merrigan

Los Alamos National Laboratory
P. O. Box 1663
Los Alamos, NM 87545
Attn: T. P. Suchocki

Los Alamos National Laboratory
P. O. Box 1663
Los Alamos, NM 87545
Attn: L. H. Sullivan

Martin Marietta Corp.
P. O. Box 179
Denver, CO 80201
Attn: R. Giellis

Martin Marietta Corp.
P. O. Box 179
Denver, CO 80201
Attn: R. Zercher
MSL8060

Massachusetts Institute of
Technology
1328 Albany Street
Cabridge, MA 02139
Attn: J. A. Bernard

NASA Lewis Research Center
21000 Brookpark Road
Cleveland, OH 44135
Attn: Barbara McKissock, MS 301-5

NASA Lewis Research Center
21000 Brookpark Road
Cleveland, OH 44135
Attn: A. Juhasz, MS 301-5

NASA Lewis Research Center
21000 Brookpark Road
Cleveland, OH 44135
Attn: J. Smith, MS 301-5

NASA Lewis Research Center
21000 Brookpark Road
Cleveland, OH 44135
Attn: H. Bloomfield, MS 301-5

NASA Lewis Research Center
21000 Brookpark Road
Cleveland, OH 44135
Attn: C. Purvis, MS 203-1

NASA Lewis Research Center
21000 Brookpark Road
Cleveland, OH 44135
Attn: D. Bents, MS 301-5

NASA Lewis Research Center
21000 Brookpark Road
Cleveland, OH 44135
Attn: I. Myers, MS 301-2

NASA Lewis Research Center
21000 Brookpark Road
Cleveland, OH 44135
Attn: G. Schwarze, MS 301-2

NASA Lewis Research Center
21000 Brookpark Road
Cleveland, OH 44135
Attn: J. Sovie, MS 301-5

NASA Lewis Research Center
21000 Brookpark Road
Cleveland, OH 44135
Attn: Barbara Jones, MS 301-5

National Research Council
Energy Engineering Board
Commission on Engineering
and Technical Systems
2101 Constitution Avenue
Washington, DC 20418
Attn: R. Cohen

Naval Research Laboratory
Washington, DC 20375-5000
Attn: R. L. Eilbert

Naval Research Laboratory
Washington, DC 20375-5000
Attn: I. M. Vitkovitsky

Naval Space Command
Dahlgren, VA 22448
Attn: Commander R. Nosco

Naval Space Command
N5
Dahlgren, VA 22448
Attn: Maj. J. Wiley

Naval Space Command
Dahlgren, VA 22448
Attn: Mr. B. Meyers

Naval Surface Weapons Center
Dahlgren, VA 22448-5000
Attn: R. Gripshoven-F12

Naval Surface Weapons Center
Dahlgren, VA 22448-5000
Attn: R. Dewitt-F12

Naval Surface Weapons Center
White Oak Laboratory
Silver Springs, MD 20903-500
MC R-42
Attn: B. Maccabee

Nichols Research Corp.
2340 Alamo Street, SE
Suite 105
Albuquerque, NM 87106
Attn: R. Weed

Oak Ridge National Laboratory
P. O. Box Y
Bldg. 9201-3, MS-7
Oak Ridge, TN 37831
Attn: J. P. Nichols

Oak Ridge National Laboratory
P. O. Box Y
Bldg. 9201-3, MS-7
Oak Ridge, TN 37831
Attn: D. Bartine

Oak Ridge National Laboratory
P. O. Box X
Oak Ridge, TN 37831
Attn: H. W. Hoffman

Oak Ridge National Laboratory
P. O. Box Y
Bldg. 9201-3, MS-7
Oak Ridge, TN 37831
Attn: R. H. Cooper, Jr.

Oak Ridge National Laboratory
P. O. Box Y
Bldg. 9201-3, MS-7
Oak Ridge, TN 37831
Attn: J. C. Moyers

Oak Ridge National Laboratory
P. O. Box Y
Oak Ridge, TN 37831
Attn: M. Olszewski

Oak Ridge National Laboratory
P. O. Box Y
Bldg. 9201-3, MS-7
Oak Ridge, TN 37831
Attn: M. Siman-Tov

Oak Ridge National Laboratory
P. O. Box Y
Bldg. 9201-3, MS-7
Oak Ridge, TN 37831
Attn: F. W. Wiffen

RADC/OCTP
Griffiss AFB
New York 13441
Attn: R. Gray

Riverside Research Institute
1701 No. Ft. Meyers Drive
Suite 700
Arlington, VA 22209
Attn: J. Feig

Science Applications, Inc.
505 Marquette Avenue NW
Albuquerque, NM 87102
Attn: D. Buden

Science & Engineering Associates
6301 Indian School Road, NE
Albuquerque, NM 87110
Attn: G. L. Zigler

SDI Organization
The Pentagon
Washington, DC 20301-7100
Attn: R. Verga

SDI Organization
The Pentagon
Washington, DC 20301-7100
Attn: R. Wiley

SDI/SLKT
The Pentagon
1717 H. St. NW
Washington, D. C. 20301
Attn: C. Northrup

SDIO/DE
Washington, DC 20301-7100
Attn: Dr. J. Hammond

SDIO/IST
Washington, DC 20301-7100
Attn: Dr. L. Cavery

SDIO/KE
The Pentagon
Washington, DC 20301-7100
Attn: Col. R. Ross

SDIO/KE
The Pentagon
Washington, DC 20301-7100
Attn: Maj. R. X. Lenard

SDIO/SATKA
Washington, DC 20301-7100
Attn: Col. Garry Schnelzer

SDIO/SY
Washington, DC 20301-7100
Attn: Dr. C. Sharn

SDIO/SY
Washington, DC 20301-7100
Attn: Col. J. Schofield

SDIO/SY
Washington, DC 20301-7100
Attn: Col. J. Graham

SDIO/SY
Washington, DC 20301-7100
Attn: Capt. J. Doegan

Space Power, Inc.
253 Humbolt Court
Sunnyvale, CA 94089
Attn: J. R. Wetch

State University of New York
at Buffalo
Dept. of Elec. Engineering
312 Bonner Avenue
Buffalo, NY 14260
Attn: Jim Sargeant

TRW
One Space Park
Redondo Beach, CA 90278
Attn: R. Hammel

TRW
One Space Park
Redondo Beach, CA 90278
Attn: T. Fitzgerald

TRW
One Space Park
Redondo Beach, CA 90278
Attn: C. Garner

TRW-ATD
One Space Park
Redondo Beach, CA 90278
Attn: B. Glasgow

TRW
One Space Park
Redondo Beach, CA 90278
Attn: A. D. Schoenfeld

Teledyne Brown Engineering
Cummings Research Park
Huntsville, AL 35807
Attn: Dan DeLong

Texas A&M University
Nuclear Engineering Dept.
College Station, TX 77843-3133
Attn: F. Best

Texas Tech. University
Dept. of Electrical Engr.
Lubbock, TX 79409
Attn: Dr. W. Portnoy

U. S. Army ARDC
Building 329
Picatinny Arsenal
New Jersey 87806-5000
Attn: SMCAR-SSA-E

U. S. Army Belvoir RDE Center
Fort Belvoir, VA 22060-5606
Attn: Dr. L. Amstutz-STRABE-FGE

U. S. Army Lab. Com.
SLKET/ML
Pulse Power Technology Branch
Fort Monmouth, NJ 07703-5000
Attn: S. Levy

U. S. Army Lab. Com.
SLKET/ML
Pulse Power Technology Branch
Fort Monmouth, NJ 07703-5000
Attn: N. Wilson

U. S. Army Strategic Defense Com.
106 Wynn Drive
Huntsville, AL 35807
Attn: C. Cooper

U. S. Army Strategic Defense Com.
106 Wynn Drive
Huntsville, AL 35807
Attn: G. Edlin

U. S. Army Strategic Defense Com.
106 Wynn Drive
Huntsville, AL 35807
Attn: R. Hall

U. S. Army Strategic Defense Com.
106 Wynn Drive
Huntsville, AL 35807
Attn: E. L. Wilkinson

U. S. Army Strategic Defense Com.
106 Wynn Drive
Huntsville, AL 35807
Attn: D. Bouska

U. S. Army Strategic Defense Com.
106 Wynn Drive
Huntsville, AL 35807
Attn: W. Sullivan

U. S. Army Strategic Defense Com.
106 Wynn Drive
Huntsville, AL 35807
Attn: F. King

U. S. Department of Energy
Chicago Operations Office
9800 S. Cass Avenue
Argonne, IL 60439
Attn: J. L. Hooper

U. S. Department of Energy
NE-52
GTN
Germantown, MD 20545
Attn: J. Warren

U. S. Department of Energy
NE-54
F415/GTN
Germantown, MD 20545
Attn: E. Wahlquist

U. S. Department of Energy
NE-521
Germantown, MD 20874
Attn: D. Bennett

U. S. Department of Energy
San Francisco Operations Office
1333 Broadway Ave,
Oakland, CA 94612
Attn: J. K. Hartman

U. S. Department of Energy
SAN - ACR Division
1333 Broadway
Oakland, CA 94612
Attn: J. Krupa

U. S. Department of Energy
SAN - ACR Division
1333 Broadway
Oakland, CA 94612
Attn: W. Lambert

U. S. Department of Energy
SAN - ACR Division
1333 Broadway
Oakland, CA 94612
Attn: J. Zielinski

U. S. Department of Energy
Pittsburgh Energy Tech. Center
P.O. Box 18288
Pittsburgh, PA 15236
Attn: G. Staats (PM-20)

U. S. Department of Energy
NE-54
Washington, DC 20545
Attn: I. Helms

U. S. Department of Energy
Oak Ridge Operations Office
P.O. Box E
Oak Ridge, TN 37830
Attn: E. E. Hoffman

U. S. Department of Energy
Washington, DC 20545
Attn: S. J. Lanes

U. S. Department of Energy
MA 206
Washington, DC 20545
Attn: J. P. Lee

U. S. Department of Energy
San Francisco Operations Office
1333 Broadway Avenue
Oakland, CA 94612
Attn: S. L. Samuelson

U. S. Department of Energy
ALO/ETD
P.O. Box 5400
Albuquerque, New Mexico 87115
Attn: R. Holton

U. S. Department of Energy
ALO/ETD
P.O. Box 5400
Albuquerque, New Mexico 87115
Attn: C. Quinn

U. S. Department of Energy/Idaho
785 DOE Place
Idaho Falls, ID 83402
Attn: P. J. Dirkmaat

United Technologies
International Fuel Cells
195 Governor's Highway
South Windsor, CT 06074
Attn: D. McVay

United Technologies
International Fuel Cells
195 Governor's Highway
South Windsor, CT 06074
Attn: J. L. Preston, Jr.

United Technologies
International Fuel Cells
195 Governor's Highway
South Windsor, CT 06074
Attn: J. C. Trocciola

University of Missouri - Rolla
220 Engineering Research Lab
Rolla, MO 65401-0249
Attn: A. S. Kumar

University of New Mexico
Chemical and Nuclear Eng. Department
Albuquerque, NM 87131
Attn: M. El-Genk

University of Wisconsin
Fussion Technology Institute
1500 Johnson Drive
Madison, WI 53706-1687
Attn: Gerald Kukinski

W. J. Schafer Associates
1901 No. Ft. Myers Drive
Suite 800
Arlington, VA 22209
Attn: P. Mace

W. J. Schafer Associates
1901 No. Ft. Myers Drive
Suite 800
Arlington, VA 22209
Attn: S. Bassett

W. J. Schafer Associates
1901 No. Ft. Myers Drive
Suite 800
Arlington, VA 22209
Attn: M. Nikolich

W. J. Schafer Associates
1901 No. Ft. Myers Drive
Suite 800
Arlington, VA 22209
Attn: J. Crissey

W. J. Schafer Associates
2000 Randolph Road, SE
#205
Albuquerque, NM 87106
Attn: D. C. Straw

W. J. Schafer Associates
1901 No. Ft. Myers Drive
Suite 800
Arlington, VA 22209
Attn: A. K. Hyder

Westinghouse Electric
P. O. Box 158
Madison, PA 15663-0158
Attn: J. Chi

Westinghouse
Advanced Energy Systems Division
Manager, Space & Defense Program
Route 70, Madison Exit
Madison, PA 15663
Attn: J. F. Wett

Westinghouse
Advanced Energy Systems Division
P.O. Box 158
Madison, PA 15663
Attn: Dr. J. W. H. Chi

Westinghouse R&D
1310 Beulah Road
Bldg. 501-3Y56
Pittsburgh, PA 15235
Attn: J. R. Repp

Westinghouse R&D
1310 Beulah Road
Bldg. 501-3Y56
Pittsburgh, PA 15235
Attn: L. Long

Westinghouse R&D
1310 Beulah Road
Bldg. 501-3Y56
Pittsburgh, PA 15235
Attn: Owen Taylor

Westinghouse Advanced Energy
Systems Division
P. O. Box 158
Madison, PA 15663
Attn: G. Farbman

Westinghouse Hanford Co.
P. O. Box 1970
Richland, WA 99352
Attn: D. S. Dutt

Westinghouse Hanford Co.
P. O. Box 1970
Richland, WA 99352
Attn: B. J. Makenas

1140 P. S. Peercy
1200 J. P. Van Devender
1240 K. R. Prestwich
1248 M. T. Buttram
1261 M. J. Clauser
1270 R. B. Miller
1513 D. J. Rader
1800 R. L. Schwoebel
1810 R. G. Kepler
1830 M. J. Davis
1832 W. B. Jones
1832 R. J. Salzbrenner
1840 R. J. Eagan
2110 R. E. Bair
2120 E. G. Franzek
2180 C. F. Gibbon
2150 E. D. Graham, Jr.
2560 J. T. Cutchen
3141 S. A. Landenberger (5)
3151 W. L. Garner (3)
3154-1 C.H. Dalin
(28 for DOE/OSTI)
6400 D. J. McCloskey
6410 N. R. Ortiz
6416 J. S. Philbin
6420 J. V. Walker
6421 P. S. Pickard
6422 J. E. Brockmann
6425 W. J. Camp
6440 D. A. Dahlgren
6450 T. R. Schmidt
6500 A. W. Snyder
6510 W. B. Gauster
6511 L. O. Cropp
6511 M. W. Edenburn
6511 D. R. Gallup
6511 S. L. Hudson
6511 A. C. Marshall
6511 W. H. McCulloch
6511 R. E. Pepping
6511 F. V. Thome
6512 D. M. Ericson, Jr. (5)
6512 M. S. Chu
6512 V. J. Dandini
6512 D. Dobranich (10)
6512 P. J. McDaniel
6512 F. J. Wyant
8024 P. W. Dean
8400 R. C. Wayne
9000 R. L. Hagengruber
9010 W. C. Hines
9012 J. W. Keizur
9012 L. W. Connell
9012 R. M. Zazworsky
9100 R. G. Clem
9110 P. A. Stokes
9140 D. J. Rigali